Article

RNAseq Analysis of FABP4 Knockout Mouse Hippocampal Transcriptome Suggests a Role for WNT/β-Catenin in Preventing Obesity-Induced Cognitive Impairment

Simon W. So [1,2], Joshua P. Nixon [1,3,4], David A. Bernlohr [5] and Tammy A. Butterick [1,2,3,*]

1   Minneapolis Veterans Affairs Health Care System, Minneapolis, MN 55417, USA
2   Department of Neuroscience, University of Minnesota Twin Cities, Minneapolis, MN 55455, USA
3   Department of Food Science and Nutrition, University of Minnesota Twin Cities, St. Paul, MN 55108, USA
4   Department of Surgery, University of Minnesota Medical School, Minneapolis, MN 55455, USA
5   Department of Biochemistry, Molecular Biology, and Biophysics, University of Minnesota Twin Cities, Minneapolis, MN 55455, USA
*   Correspondence: butte017@umn.edu

Abstract: Microglial fatty-acid binding protein 4 (FABP4) is a regulator of neuroinflammation. We hypothesized that the link between lipid metabolism and inflammation indicates a role for FABP4 in regulating high fat diet (HFD)-induced cognitive decline. We have previously shown that obese FABP4 knockout mice exhibit decreased neuroinflammation and cognitive decline. FABP4 knockout and wild type mice were fed 60% HFD for 12 weeks starting at 15 weeks old. Hippocampal tissue was dissected and RNA-seq was performed to measure differentially expressed transcripts. Reactome molecular pathway analysis was utilized to examine differentially expressed pathways. Results showed that HFD-fed FABP4 knockout mice have a hippocampal transcriptome consistent with neuroprotection, including associations with decreased proinflammatory signaling, ER stress, apoptosis, and cognitive decline. This is accompanied by an increase in transcripts upregulating neurogenesis, synaptic plasticity, long-term potentiation, and spatial working memory. Pathway analysis revealed that mice lacking FABP4 had changes in metabolic function that support reduction in oxidative stress and inflammation, and improved energy homeostasis and cognitive function. Analysis suggested a role for WNT/β-Catenin signaling in the protection against insulin resistance, alleviating neuroinflammation and cognitive decline. Collectively, our work shows that FABP4 represents a potential target in alleviating HFD-induced neuroinflammation and cognitive decline and suggests a role for WNT/β-Catenin in this protection.

Keywords: obesity; transcriptome; hippocampus; long-term potentiation; cognitive decline; inflammation; microglia; WNT/β-Catenin

1. Introduction

Midlife obesity is associated with earlier onset of Alzheimer's disease (AD) and increased AD neuropathology [1–3]. Obesity is often characterized by chronic low-level inflammation, along with metabolic disorders such as type-2 diabetes mellitus and insulin resistance [4–6]. Insulin resistance is accompanied by increased fatty acid transport and circulation. Fatty acid binding protein 4 (FABP4; also known as adipocyte protein-2; aP2) is a fatty acid binding protein with roles in fatty acid transport and lipid metabolism. FABP4 knockout in adipocytes is associated with reduced inflammation, insulin resistance, and metabolic dysfunction [7]. Overconsumption of a high fat diet (HFD), specifically those rich in saturated fatty acids (SFA), has been shown to exacerbate neuroinflammation, neurodegeneration, and cognitive impairment [4,6,8–15]. Studies indicate that this is influenced more by dietary SFA content than by total calories consumed [4,15].

The FABP4 knockout mouse model (AKO) has allowed an increasingly comprehensive understanding of lipid metabolism, diabetes, and peripheral immune response [16–20]. Unlike obese wild type controls, AKO mice present with decreased TNF-α (a biomarker of obesity-related insulin resistance) in adipose tissue [5]. Fatty acid metabolism plays a central role in immunometabolic diseases, including diet-induced obesity and metabolic syndrome [16,21,22]. We hypothesized that the link between lipid metabolism and inflammation indicates a role for FABP4 in regulating HFD-induced cognitive decline. We have previously shown that AKO mice are protected against HFD-induced hippocampal proinflammatory cytokine expression and memory deficits [23,24]. These mice were fed HFD for 12 weeks starting at 15 weeks of age. Herein, we investigated the transcriptomics of the AKO model fed HFD compared to wild type (WT) mice fed the same diet. As our previous research showed no differences in hippocampal inflammation and cognitive decline between groups fed normal chow diet (NC), nor between HFD-fed and NC-fed AKO groups [23], only HFD hippocampal transcriptomes were analyzed. Our present results show that AKO mice present with a neuroprotective hippocampal transcriptome that correlates with a decrease in proinflammatory signaling, ER stress, apoptosis, and cognitive decline, and an increase in neurogenesis, synaptic plasticity, long-term potentiation, and spatial working memory. This is accompanied by an increase in WNT/β-Catenin signaling, suggesting a role for the pathway in preventing HFD-induced neuroinflammation and cognitive decline.

2. Results

2.1. Transcript Analysis

We determined the transcripts that were differentially expressed in HFD-fed AKO mice compared to HFD-fed WT mice. AKO and WT mice were fed 60% HFD for 12 weeks starting at 15 weeks of age. Hippocampal tissue was dissected and RNAseq was performed to measure differentially expressed transcripts. Transcript analysis showed 1793 differentially expressed transcripts at log10 adjusted *p*-value (*p*adj) ≤ 0.05 (Figure 1).
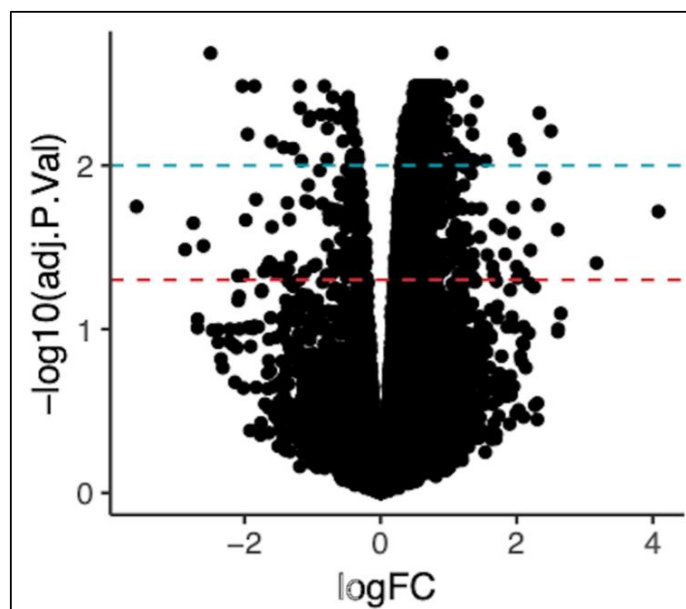

Figure 1. Volcano plot of the distribution of magnitude and significance of all genes. Log fold change (log2) is represented on the *x*-axis. Significance (log10 adjusted *p*-value) is represented on the *y*-axis. The red line indicates *p*adj = 0.05 and the blue line indicates *p*adj = 0.01.

2.2. Downregulated Transcripts in HFD-Fed AKO Compared to HFD-Fed WT Mice

We determined the transcripts that were most downregulated in HFD-fed AKO mice compared to HFD-fed WT mice (LFC ≤ -1.00, *p*adj ≤ 0.001). There were 12 transcripts

in total (Table 1). HFD-fed AKO mice have downregulated transcripts associated with negative regulation of Wnt/β-Catenin signaling [25] and neurite outgrowth [26] along with positive regulation of cognitive decline [27], proinflammatory cytokine signaling [28,29], amyloid beta plaque formation [30], and ER stress [31]. Downregulated transcripts also have roles associated with lipid metabolism [32] and GABA signaling [33,34].

Table 1. Downregulated Transcripts in HFD-fed AKO Compared to HFD-fed WT Mice. Transcripts with LFC ≤ −1.00 and $p$adj ≤ 0.001 are displayed. Gene symbol, Ensembl ID, gene description, log fold change (log2), log10 adjusted p-value, and relevant known function are displayed.

Gene Symbol	Ensembl ID	Gene Description	Log FC	$p$adj	Function
Fabp4	ENSMUST00000029041	Fatty acid binding protein 4, adipocyte	−2.50	2.06×10^{-3}	Positive regulator of obesity linked inflammation and ER stress [20]
Sox6	ENSMUST00000072804	SRY (sex determining region Y)-box 6	−2.03	3.27×10^{-3}	Negative regulator of Wnt/β-catenin signaling [25]
Apoa2	ENSMUST00000005824	Apolipoprotein A-II	−1.95	6.44×10^{-3}	Component of HDL with role in lipid metabolism and positive regulator of amyloidosis [32], Positively associated with cognitive decline [27]
Ube3a	ENSMUST00000202945	Ubiquitin protein ligase E3A	−1.85	3.27×10^{-3}	Positive regulator of amyloid plaque formation [30], Positive regulator of GABA release [33]
Tpx2	ENSMUST00000028969	TPX2-microtubule associated	−1.61	7.15×10^{-3}	Positive regulator of proinflammatory cytokines [28]
Dmd	ENSMUST00000114000	Dystrophin, muscular dystrophy	−1.43	7.76×10^{-3}	Positive regulator of proinflammatory cytokines [29], Associated with altered GABA signaling [35]
Eif4e2	ENSMUST00000113233	Eukaryotic translation initiation factor 4E member 2	−1.29	7.88×10^{-3}	Phosphorylated state is positively associated with hyperphosphorylated tau and AD [36]
Zfp971	ENSMUST00000108926	Zinc finger protein 971	−1.19	3.27×10^{-3}	Unknown function, predicted to increase DNA-binding transcription repressor activity [37], contains KRAB box and C2H2 type domain [38], may have a role in neurodegenerative diseases [39]
Zwint	ENSMUST00000105431	ZW10 interactor	−1.18	4.46×10^{-3}	Associated protein has role in retrograde trafficking from Golgi to ER [34]
Tmod2	ENSMUST00000164100	Tropomodulin 2	−1.17	9.35×10^{-3}	Negative regulator of neurite outgrowth [26]
Lonp2	ENSMUST00000155433	lon peptidase 2, peroxisomal	−1.05	5.32×10^{-3}	Upregulated in response to ER stress [31]
Wtap	ENSMUST00000159986	Wilms tumour 1 -associating protein	−1.04	5.05×10^{-3}	Positive regulator of m6A methylation [40] promoting AD development [41]

2.3. Upregulated Transcripts in HFD-Fed AKO Compared to HFD-Fed WT Mice

We determined the transcripts that were most upregulated in HFD-fed AKO mice compared to HFD-fed WT mice (LFC $\geq$ 1.00, *p*adj $\leq$ 0.001). There were 19 transcripts in total (Table 2). AKO mice fed HFD have upregulated transcripts associated with negative regulation of apoptosis [42–44], neuroinflammation [45], and ER stress [42,43] along with positive regulation of long-term potentiation [46–48], spatial working memory [49], synaptic plasticity [50,51], neurogenesis [52,53], and Wnt/β-Catenin signaling [54].

Table 2. Upregulated Transcripts in HFD-fed AKO Compared to HFD-fed WT Mice. Transcripts with LFC $\geq$ 1.00 and *p*adj $\leq$ 0.001 are displayed. Gene symbol, Ensembl ID, gene description, log fold change (log2), log10 adjusted *p*-value, and relevant known function are displayed.

Gene Symbol	Ensembl ID	Gene Description	Log FC	*p*adj	Function
Sort1	ENSMUST00000135636	Sortilin 1	1.007	3.53×10^{-3}	Positive regulator of murine apoE clearance in brain [55], Regulator of lipid metabolism in brain [56]
Hspa5	ENSMUST00000100171	Heat shock protein 5	1.038	9.34×10^{-3}	Antiapoptotic regulator of ER stress and unfolded protein response [42]
Adra2a	ENSMUST00000237285	Adrenergic receptor, alpha 2a	1.069	7.32×10^{-3}	Positive regulator of NMDA receptor-dependent long-term potentiation [46]
Atp2a2	ENSMUST00000031423	ATPase, Ca++ transporting, cardiac muscle, slow twitch 2	1.103	5.32×10^{-3}	Regulator of calcium homeostasis [57], Downregulated in AD brain [58]
S1pr3	ENSMUST00000087978	Sphingosine-1-phosphate receptor 3	1.144	8.07×10^{-3}	Negative regulator of inflammation in brain [45], Positive regulator of spatial working memory [49]
Mdga1	ENSMUST00000171691	MAM domain containing glycosylphos-phatidylinositol anchor 1	1.151	8.87×10^{-3}	Positive regulator of hippocampal long-term potentiation [47], Regulator of trans-synaptic bridge formation [59]
H3c15	ENSMUST00000167403	H3 clustered histone 15	1.193	3.27×10^{-3}	Associated with the formation of the β-catenin:TCF transactivating complex and Senescence-Associated Secretory Phenotype (SASP) [60]
Paqr3	ENSMUST00000069453	Progestin and adipoQ receptor family member III	1.226	8.60×10^{-3}	Regulator of cholesterol homeostasis [61], Regulator of autophagy [62]
Brd1	ENSMUST00000109380	Bromodomain containing 1	1.317	5.30×10^{-3}	Positive regulator of H3K14 acetylation [63] associated with synaptic plasticity [50]
Gpr68	ENSMUST00000110066	G protein-coupled receptor 68	1.351	6.44×10^{-3}	Positive regulator of adult hippocampal neurogenesis [52]

Table 2. *Cont.*

Gene Symbol	Ensembl ID	Gene Description	Log FC	$p$adj	Function
Sufu	ENSMUST00000111867	SUFU negative regulator of hedgehog signaling	1.355	9.26×10^{-3}	Positive regulator of adult hippocampal neurogenesis [53]
Grm1	ENSMUST00000105560	Glutamate receptor, metabotropic 1	1.378	9.34×10^{-3}	Positive regulator of pyramidal neuron excitation [64]
Nsd3	ENSMUST00000146919	Nuclear receptor binding SET domain protein 3	1.412	4.06×10^{-3}	Positive regulator of REST mediated H3K36 trimethylation and associated with antiapoptotic genes [65]
Dlgap1	ENSMUST00000155016	DLG associated protein 1	1.538	9.33×10^{-3}	Positive regulator of synaptic scaling in excitatory synapses [51]
Grik2	ENSMUST00000105484	Glutamate receptor, ionotropic, kainate 2 (beta 2)	1.969	7.15×10^{-3}	Positive regulator of NMDA receptor-independent and KA receptor-dependent hippocampal long-term potentiation [48]
Fbxw7	ENSMUST00000107678	F-box and WD-40 domain protein 7	1.976	6.95×10^{-3}	Negatively associated with glutamate mediated excitotoxicity and negative regulator of pro-apoptotic protein c-Jun [66]
Nox1	ENSMUST00000033610	NADPH oxidase 1	2.038	8.04×10^{-3}	Positive regulator of Wnt/β-catenin signaling [54], Positive regulator of M2-type macrophage polarization [67]
Smpd4	ENSMUST00000090159	Sphingomyelin phosphodiesterase 4	2.334	4.77×10^{-3}	Negatively associated with ER stress and apoptosis in brain [43]
Zfp329	ENSMUST00000121215	Zinc finger protein 329	2.502	6.16×10^{-3}	Ortholog is a positive regulator of antiapoptotic protein BCL2 [44]

2.4. Differentially Expressed Pathways in HFD-Fed AKO Compared to HFD-Fed WT Mice

Using Reactome molecular pathway analysis, we determined the differentially expressed pathways in HFD-fed AKO mice compared to HFD-fed WT mice (FDR ≤ 0.01). There were 39 pathways in total. Nine of these pathways were unrelated to ribosomal protein subunits and were examined further for transcript function (Supplemental Table S1). We further condensed these results into pathways that relate to metabolism and Wnt/β-Catenin signaling (Table 3). Transcripts associated with the electron transport chain [68–75] and citric acid cycle [76–79] were downregulated and upregulated, respectively. Transcripts relating to Wnt/β-Catenin signaling were upregulated [80–85].

Table 3. Differentially Expressed Pathways in HFD-fed AKO Compared to HFD-fed WT Mice. FDR $\leq$ 0.01. Pathway name, stable identifier, log fold change (log2), and false discovery rate for each pathway are displayed. Within each pathway, gene ID, Ensembl ID, gene description, log fold change (log2), log10 adjusted *p*-value, and relevant known function are displayed.

Reactome Pathway	Gene Symbol	Ensembl ID	Gene Description	Log FC	*p*adj	Known Function
The citric acid (TCA) cycle and respiratory electron transport (R-HSA-1428517) LFC: 0.03 FDR: 2.71×10^{-3}	*Ndufb2* *Ndufb4* *Ndufb11* *Ndufs8* *Ndufa4* *Ndufb9* *Ndufa2*	ENSMUST00 000119379 ENSMUST00 000023514 ENSMUST00 000116621 ENSMUST00 000237341 ENSMUST00 000204978 ENSMUST00 000022980 ENSMUST00 000014438	NADH:ubiquinone oxidoreductase subunit B2 NADH:ubiquinone oxidoreductase subunit B4 NADH:ubiquinone oxidoreductase subunit B11 NADH:ubiquinone oxidoreductase core subunit S8 Ndufa4, mitochondrial complex associated NADH:ubiquinone oxidoreductase subunit B9 NADH:ubiquinone oxidoreductase subunit A2	−0.32 −0.29 −0.28 −0.27 −0.25 −0.23 −0.20	2.39×10^{-2} 2.89×10^{-2} 3.32×10^{-2} 4.63×10^{-2} 4.69×10^{-2} 4.16×10^{-2} 4.83×10^{-2}	Partial inhibition of Complex I leads to reduced oxidative stress and increased long-term potentiation in AD mice [68]
	Cox7b	ENSMUST00 000033582	Cytochrome c oxidase subunit 7B	−0.31	1.13×10^{-2}	Loss leads to decrease in oxidative stress and amyloid formation in AD mice [71]
	Uqcrh	ENSMUST00 000078676	Ubiquinol-cytochrome c reductase hinge protein	−0.29	3.04×10^{-2}	Positive regulator of apoptosis via cytochrome c release [72]
	Atp5j2 *Atp5h*	ENSMUST00 000161741 ENSMUST00 000043931	ATP synthase, H+ transporting, mitochondrial F0 complex, subunit F2 ATP synthase, H+ transporting, mitochondrial F0 complex, subunit D	−0.27 −0.26	1.82×10^{-2} 3.98×10^{-2}	Inhibition is neuroprotective in aging and AD [86]
	mt-Nd3	ENSMUST00 000082411	Mitochondrially encoded NADH dehydrogenase 3	−0.23	4.06×10^{-2}	Partial inhibition of Complex I leads to reduced oxidative stress and increased long-term potentiation in AD mice [68]
	mt-Co3	ENSMUST00 000082409	Mitochondrially encoded cytochrome c oxidase III	−0.21	3.87×10^{-2}	Loss leads to decrease in oxidative stress and amyloid formation in AD mice [71]

Table 3. *Cont.*

Reactome Pathway	Gene Symbol	Ensembl ID	Gene Description	Log FC	*p*adj	Known Function
	mt-Cytb	ENSMUST00 000082421	Mitochondrially encoded cytochrome b	0.21	4.53×10^{-2}	Decreased in AD brain [73]
	Acad9	ENSMUST00 000011492	Acyl-Coenzyme A dehydrogenase family, member 9	0.29	2.59×10^{-2}	Role in fatty acid oxidation, downregulation associated with neurological disease [69]
	Aco2	ENSMUST00 000023116	Aconitase 2, mitochondrial	0.29	1.42×10^{-2}	Suppressed by nitric oxide (Palmieri et al., 2020), Decreased in AD patient lymphocytes [76]
	Sdha	ENSMUST00 000022062	Succinate dehydrogenase complex, subunit A, flavoprotein (Fp)	0.29	1.02×10^{-2}	Downregulation is associated with oxidative stress and insulin resistance [74]
	Ogdh	ENSMUST00 000003461	Oxoglutarate (alpha-ketoglutarate) dehydrogenase (lipoamide)	0.30	3.73×10^{-2}	Inhibited by lipopolysaccharide and IFN-γ stimulation in macrophages [77]
	Cs	ENSMUST00 000005826	Citrate synthase	0.32	1.53×10^{-2}	Downregulated in AD patient platelets [78]
	Pdk2	ENSMUST00 000038431	Pyruvate dehydrogenase kinase, isoenzyme 2	0.35	4.52×10^{-2}	mRNA levels modulated during aging in brain [79]
	Timmdc1	ENSMUST00 000002925	Translocase of inner mitochondrial membrane domain containing 1	0.36	9.17×10^{-3}	Loss is associated with axonal neuropathy and cognitive decline [70]
	Taco1	ENSMUST00 000002048	Translational activator of mitochondrially encoded cytochrome c oxidase I	0.40	3.68×10^{-2}	Loss associated with motor disfunction and mitochondrial disease in mice [75]

Table 3. *Cont.*

Reactome Pathway	Gene Symbol	Ensembl ID	Gene Description	Log FC	$p$adj	Known Function
Disassembly of the destruction complex and recruitment of AXIN to the membrane (R-HSA-4641262) LFC: 0.38 FDR: 7.21×10^{-3}	*Ppp2cb* *Ppp2r5a* *Ppp2r5e* *Ppp2r1a*	ENSMUST00 000009774 ENSMUST00 000067976 ENSMUST00 000021447 ENSMUST00 000007708	Protein phosphatase 2 (formerly 2A), catalytic subunit, beta isoform Protein phosphatase 2, regulatory subunit B′, alpha Protein phosphatase 2, regulatory subunit B′, epsilon Protein phosphatase 2, regulatory subunit A, alpha	0.25 0.26 0.31 0.37	1.94×10^{-2} 4.25×10^{-2} 2.85×10^{-2} 3.87×10^{-2}	Positive regulator of Wnt/β-catenin signaling [80], Inhibition leads to spatial memory impairment [81]
	Csnk1a1 *Csnk1g2*	ENSMUST00 000165123 ENSMUST00 000085435	Casein kinase 1, alpha 1 Casein kinase 1, gamma 2	0.26 0.33	3.90×10^{-2} 4.73×10^{-2}	Negative regulators of SMAD3 and TGF-β signaling [82]
	Ctnnb1	ENSMUST00 000007130	Catenin (cadherin associated protein), beta 1	0.37	1.38×10^{-2}	Positive regulator of Wnt/β-catenin signaling, neuronal survival and synaptic plasticity, negative regulator of Aβ production [83]
	Gsk3b	ENSMUST00 000023507	Glycogen synthase kinase 3 beta	0.52	3.62×10^{-3}	Regulator of Wnt/β-catenin signaling, loss leads to synaptic and social defects in mice [84]
	Dvl3	ENSMUST00 000003318	Dishevelled segment polarity protein 3	0.72	2.23×10^{-2}	Positive regulator of Wnt/β-catenin signaling, downregulated in AD brain [83]
	Fzd1	ENSMUST00 000054294	Frizzled class receptor 1	0.73	3.81×10^{-3}	Positive regulator of Wnt/β-catenin signaling, loss leads to impairment of neuronal differentiation [85]

2.5. Differentially Expressed Microglial Markers in HFD-Fed AKO Compared to HFD-Fed WT Mice

We determined the differentially expressed transcripts that have been identified as microglial markers ($p$adj ≤ 0.05). There were 10 transcripts in total (Table 4). AKO mice fed HFD have transcripts associated with microglial markers differentially expressed. Upregulated transcripts have roles in the regulation of M2 microglial transcriptome activation [87], ER/Golgi transport [88,89], dopaminergic neuronal survival [90], FcγR-dependent phagocytosis [91], and long-term potentiation [92,93].

Table 4. Differentially Expressed Microglial Markers in HFD-fed AKO Compared to HFD-fed WT Mice. Transcripts with $p$adj $\leq$ 0.05 are displayed. Gene symbol, Ensembl ID, gene description, log fold change (log2), log10 adjusted p-value, and relevant known function are displayed.

Gene Symbol	Ensembl ID	Gene Description	Log FC	$p$adj	Function
Hpgd	ENSMUST00000034026	Hydroxyprostaglandin dehydrogenase 15 (NAD)	−0.337	3.60×10^{-2}	Increased in aged tissues and negative regulator of PGE2 signaling [94]
Cx3cr1	ENSMUST00000064165	Chemokine (C-X3-C motif) receptor 1	0.393	1.08×10^{-2}	Decreased in hippocampal tissue of diet-induced obese mice [95], Positive regulator of hippocampal long-term potentiation [92]
Cd68	ENSMUST00000018918	CD68 antigen	0.441	2.42×10^{-2}	Marker of M1 and M2 microglial activation [96]
Csf1r	ENSMUST00000025523	Colony stimulating factor 1 receptor	0.530	9.83×10^{-3}	Receptor of positive regulator of M2 microglia transcriptome [87]
Cyth4	ENSMUST00000043069	Cytohesin 4	0.571	1.90×10^{-2}	Positive regulator of ARF1 [88] which is a regulator of ER/Golgi transport [89]
Ccr5	ENSMUST00000111442	Chemokine (C-C motif) receptor 5	0.584	9.10×10^{-3}	Positive regulator of neuronal cell differentiation [97], Positive regulator of dopaminergic neuronal survival [90]
Pla2g15	ENSMUST00000034377	Phospholipase A2, group XV	0.611	3.81×10^{-3}	Positively associated with long-term memory and downregulated in AD brain [93]
Kcnk6	ENSMUST00000085818	Potassium inwardly rectifying channel, subfamily K, member 6	0.698	3.99×10^{-2}	Positively associated with homeostatic microglia [98]
Lcp2	ENSMUST00000052413	Lymphocyte cytosolic protein 2	0.788	3.68×10^{-2}	Positively associated with FcγR-dependent phagocytosis [91]
Blnk	ENSMUST00000054769	B cell linker	1.567	3.52×10^{-2}	Positively associated with FcγR-dependent phagocytosis [91]

2.6. β-Catenin Western Blot

We performed Western blotting for nuclear β-Catenin in HFD-fed AKO and WT mouse hippocampal tissue. Results showed that HFD-fed AKO mice had increased expression of nuclear β-Catenin compared to WT (Figure 2; p = 0.03).
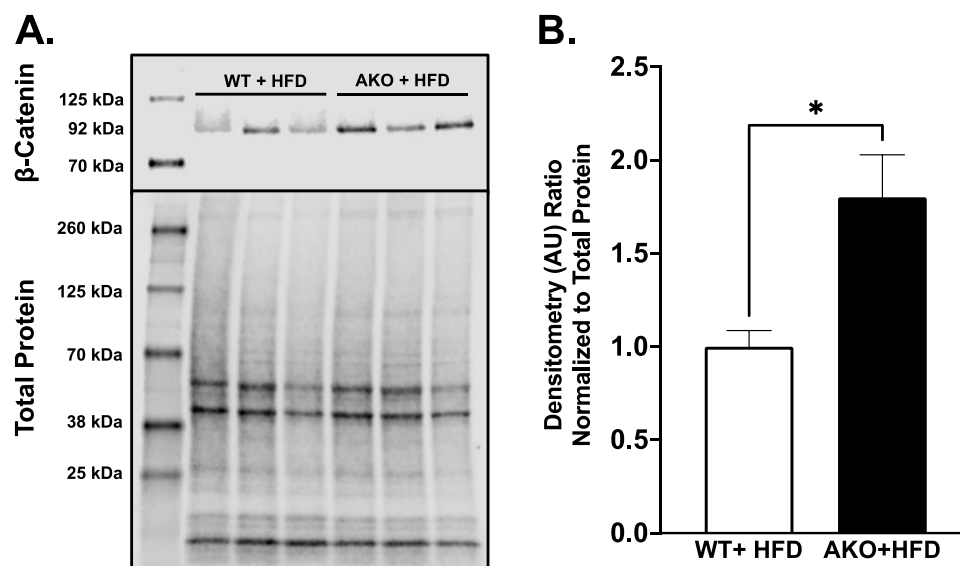
Hippocampal Nuclear β-Catenin

Figure 2. (**A**) Western blot of nuclear β-Catenin in HFD-fed AKO and WT mice. Licor Revert 700 total protein stain is shown below. (**B**) Densitometry normalized to total protein. Unpaired *t*-test, $n = 3$, * denotes significance of $p < 0.05$ ($p = 0.03$).

3. Discussion

Obesity is known to be associated with peripheral and central chronic low-grade inflammation [99]. Peripherally, HFD is linked to low-grade systemic inflammation associated with the development of metabolic disorders such as type 2 diabetes mellitus [100]. In the brain, diets high in SFAs are known to be associated with neuroinflammation, cognitive impairment, and the development of neurodegenerative diseases [101]. An increase in circulating free fatty acids (FFAs) disrupts metabolic homeostasis [102]. This increase in FFAs can also activate Toll-like receptor 4 (TLR4) in microglia, leading to ER stress and increased inflammatory cytokine expression [103]. In turn, increased ER stress and neuroinflammation can lead to cognitive deficits and neurodegenerative diseases such as AD [102]. The HFD-fed FABP4 knockout model has revealed an altered hippocampal transcriptome that is shown to have changes in metabolic pathways and be neuroprotective against HFD-induced neuroinflammation and cognitive decline.

In the present study, the AKO model has shown an altered hippocampal transcriptome with changes in metabolic pathways. AKOs had a decrease in pathways relating to the electron transport chain (ETC). These pathways were "formation of ATP by chemiosmotic coupling", "cristae formation", "complex I biogenesis", "respiratory electron transport, ATP synthesis by chemiosmotic coupling, and heat production by uncoupling proteins", and "respiratory electron transport" (Supplemental Table S1). Importantly, the major downregulated transcripts in these pathways encode for subunits of NADH:ubiquinone oxidoreductase (Complex I) and ATP synthase (Complex V) of the ETC. Partial inhibition of Complex I has been shown to improve energy homeostasis, synaptic activity, long-term potentiation, and cognitive function while reducing oxidative stress and inflammation in the brain [68]. Targeting Complex V has been shown to decrease expression of an aged and dementia-associated transcriptome [86]. AKOs had an increase in the "citric acid (TCA) cycle and respiratory electron transport" pathway (Table 3). It is important to note that transcripts relating to the tricarboxylic acid cycle (TCA) were increased. These transcripts include *Aco2*, *Cs*, *Ogdh*, and *Sdha*. Downregulation of these transcripts have been observed in neurodegenerative transcriptomes and some have been associated with oxidative stress and insulin resistance [74,76–78]. Our previous work has shown that FABP4 knockout confers protection against ROS production and ER stress through an increase

in UCP2 [20]. As such, our present results provide further evidence that FABP4 knockout leads to protective metabolic changes in HFD-fed mice. The AKO model has also shown an increase in a pathway relating to Golgi transport. This pathway is named "transport to the Golgi and subsequent modification" (Supplemental Table S1). The upregulated genes in this pathway include regulators of ER to Golgi transport [104,105] and a decrease in some of these transcripts have been associated with ER stress [106] and neurodegenerative diseases [107,108]. As Golgi function and transport is important for lipid metabolism [109], changes in transcripts relating to these pathways provide further insight on the neuroprotection conferred via FABP4 knockout. Differentially expressed genes relating to lipid metabolism in AKOs were *Apoa2* (Table 1) and *Sort1* (Table 2). *Apoa2* was downregulated in AKOs and encodes for a high-density lipoprotein. Certain polymorphisms of *Apoa2* are known to be associated with obesity [110]. *Sort1* was upregulated in AKOs and has been shown to modulate low-density lipoprotein uptake in macrophages [111]. Together, these changes in metabolic and Golgi transport pathways, along with genes associated with changes in lipid metabolism, show that HFD-fed AKO mice have a hippocampal transcriptome consistent with neuroprotection.

Previously, we have shown that HFD-fed AKO mice exhibit an alleviation of hippocampal inflammatory cytokine signaling compared to HFD-fed WT mice [23]. In the present study, HFD-fed AKO mice had transcriptome changes consistent with a decrease in neuroinflammation. AKOs had decreased expression of *Tpx2* and *Dmd* (Table 1), along with increased expression of *S1pr3* (Table 2). Silencing of *Tpx2* has been shown to decrease inflammation as marked by decreases in TNF-α, IL-6, and IL-8 protein levels [28]. Mice deficient of dystrophin, the protein encoded by *Dmd*, exhibit decreased infiltration of CD3+ T cells [29]. Knockdown of *S1pr3* has been shown to exacerbate neuroinflammation as measured by IBA1 and TNF-α [45]. HFD-fed AKO mice also had transcriptome changes consistent with a decrease in ER stress. AKOs had decreased expression of *Lonp2* (Table 1), and increased expression of *Hspa5* and *Smpd4* (Table 2). ER stress is known to cause a decrease in LONP2 expression [31]. HSPA5 is known to be a regulator of ER stress in the brain [42] and loss of SMPD4 has been shown to induce ER stress in the brain [43]. HFD is known to cause ER stress in the hippocampus [112] and ER stress can trigger inflammatory responses in the brain, leading to neurodegeneration [113]. Therefore, the transcriptomic changes relating to decreases in ER stress provide a potential mechanism for the decrease in neuroinflammation.

We have also previously shown that HFD-fed AKO mice exhibit an alleviation of cognitive decline and memory deficits compared to HFD-fed WT mice [23]. In the present study, HFD-fed AKO mice had transcriptome changes consistent with a decrease in cognitive decline. AKOs had decreased expression of *Apoa2* (Table 1). Increased APOA2 expression is associated with cognitive impairment and late-life dementia [27]. AKOs also had transcriptome changes consistent with a decrease in apoptosis. Expression of *Hspa5* and *Smpd4* were increased (Table 2). HSPA5 is known to be an antiapoptotic factor for cells undergoing ER stress [42]. Loss of SMPD4 has been shown to lead to apoptosis under stress conditions [43]. As apoptosis leading to neuronal cell death has been associated with AD pathogenesis [114], an increase in antiapoptotic factors could contribute to a neuroprotective profile against cognitive decline. AKOs also had a transcriptome negatively associated with AD. Expression of *Eif4e2* and *Wtap* were decreased (Table 1), and expression of *Atp2a2* was increased (Table 2). The phosphorylated state of EIF4E is associated with hyperphosphorylated tau and AD [36]. WTAP is a component of the complex responsible for m6A methylation [40], which is increased in AD mice [41]. Expression of ATP2A2 has been shown to be decreased in the AD brain [58]. As cognitive decline is a hallmark of AD, a transcriptome negatively associated with AD further reveals the neuroprotective profile of the AKO hippocampus.

The transcriptomic changes in HFD-fed AKO mice also reveals differentially expressed transcripts that relate to neurite outgrowth and neurogenesis. Expression of *Tmod2* was decreased (Table 1), and expression of *Gpr68* and *Sufu* were increased (Table 2). Knockdown

of *Tmod2* leads to an increase in neurite outgrowth in vitro [26]. There is evidence to show that GPR68 has a positive role in neurogenesis [52]. Deletion of *Sufu* has been shown to decrease neurogenesis in the dentate gyrus [53]. As a decrease in neurogenesis is linked to cognitive deficits and neurodegenerative disease [115], transcriptomic changes that promote neurogenesis would further confer protection against cognitive decline. HFD-fed AKO mice also had transcriptomic changes relating to synaptic plasticity and long-term potentiation. Expression of *Brd1*, *Adra2a*, *Mdga1*, and *Grik2* were increased (Table 2). The BRD1 protein is needed for H3K14 acetylation [63], which is associated with synaptic plasticity [50]. The activation of α2-adrenergic receptors has been shown to promote long-term potentiation in the mouse brain [46]. Mice lacking MDGA1 and GRIK2 have exhibited compromised hippocampal long-term potentiation [47,48]. Long-term potentiation and synaptic plasticity are critical for forming memories and preventing cognitive impairment [116]. The AKO hippocampal transcriptome further reveals protection against cognitive decline by having upregulated transcripts that promote synaptic plasticity.

The WNT/β-Catenin signaling pathway has been shown to be neuroprotective against cognitive decline and neurodegenerative disease. Mechanisms that confer this protection include increasing neuronal survival, neurogenesis, synaptic plasticity, and blood–brain barrier integrity, as well as decreasing amyloid-β production and tau hyperphosphorylation [83,117–119]. HFD-fed AKO mice exhibited transcript and pathway changes consistent with an increase in WNT/β-Catenin signaling. After *Fabp4*, the next most downregulated transcript was *Sox6* (Table 1), which has been shown to inhibit WNT/β-Catenin signaling in adipocytes [25]. The third most upregulated transcript was *Nox1* (Table 2), which has been shown to increase WNT/β-Catenin signaling [54]. Reactome analysis revealed that the most upregulated pathway was "disassembly of the destruction complex and recruitment of AXIN to the membrane" (Table 3). Within this pathway, transcripts that were increased included *Ctnnb1*, *Dvl3*, *Fzd1*, *Ppp2cb*, *Ppp2r1a*, *Ppp2r5a*, and *Ppp2r5e* (Table 3). These transcripts encode for proteins that are positive regulators of WNT/β-Catenin signaling, and have roles in neuronal survival, synaptic plasticity, neuronal differentiation, and improved spatial memory [80,83–85]. *Ccnd1*, a target of WNT/β-Catenin signaling [120], was also found to be increased in AKOs (Log FC: 0.63, *p*adj: 3.62×10^{-2}). As CCND1 has been shown to be a positive regulator of neurogenesis [121], the increase in this target gene further supports the neuroprotective profile of AKOs. To verify the increase in WNT/β-Catenin signaling, we performed Western blotting for nuclear β-Catenin in HFD-fed AKO and WT mouse hippocampal tissues. Results showed that AKO mice had an 80% increase in nuclear β-Catenin expression compared to WT (Figure 2). This is higher than the increase in *Ctnnb1* transcript, which was 30% (Table 3). These results further show that loss of FABP4 confers neuroprotection against HFD-induced cognitive decline and suggests a role for WNT/β-Catenin in this protection. It is important to note that *Csnk1a1*, *Csnk1g2*, and *Gsk3b* were also upregulated in this pathway (Table 3). These transcripts encode for proteins that are canonically negative regulators of WNT/β-Catenin signaling. These proteins are known to have roles in other pathways in the brain. Casein kinase 1 is known to be a negative regulator of TGF-β [82], whose overproduction in the brain has been linked with glucose intolerance [122]. GSK3B also has many roles in the brain including regulating neurogenesis, axon growth, and synaptic plasticity [123]. These roles may explain why these transcripts were upregulated in AKOs.

FABP4 is expressed in peripheral macrophages and microglia. In the periphery, knockout of FABP4 in macrophages leads to a decrease in inflammatory cytokine secretion [124]. We have previously shown that FABP4 is expressed in microglia [24]. As microglia activation is an important aspect of HFD-induced neuroinflammation, we decided to examine the changes in microglial marker transcripts in AKOs. The transcripts *Csf1r* and *Kcnk6* were both significantly upregulated (Table 4). *Csf1r* encodes for the receptor of colony stimulating factor 1, a positive regulator of the M2 microglial transcriptome [87]. KCNK6 is associated with a homeostatic microglial phenotype [98]. Other upregulated microglial transcripts include positive regulators of memory and long-term potentiation [92,93], and neuronal

cell differentiation and survival [90,97]. Together HFD-fed AKO mice have changes in microglial transcripts consistent with homeostatic microglia and protection against cognitive decline. Future studies will include the immunohistochemical staining of these microglial markers to provide further insight on their regulation in the AKO hippocampus.

The HFD-fed FABP4 knockout model has revealed an altered hippocampal transcriptome that is shown to have changes in metabolic pathways and be neuroprotective against HFD-induced neuroinflammation and cognitive decline. We and others have shown that knockout of FABP4 leads to an alleviation of HFD-induced peripheral and central inflammation, insulin insensitivity, and cognitive decline [16,20,23]. In the present study, we have shown that this alleviation in the brain is associated with changes in metabolic pathways, Golgi transport, and WNT/β-Catenin signaling. As there is much supporting evidence that the WNT/β-Catenin pathway is neuroprotective against cognitive decline, our study suggests a role for WNT/β-Catenin in the FABP4 knockout-induced alleviation of cognitive decline. Other studies have shown that WNT/β-Catenin has a role in the regulation of microgliosis. A decrease in WNT/β-Catenin signaling has been shown to lead to proinflammatory microglial activation in the developing brain [125]. Wnt-3a, an activator of WNT/β-Catenin signaling, causes a decrease in the expression of inducible nitric oxide synthase (iNOS) and TNF-α and a decrease in microgliosis [126], while increasing insulin sensitivity [127]. Other activators of WNT/β-Catenin signaling have been shown to cause a switch in microglia from a proinflammatory phenotype to an anti-inflammatory one after ischemic stroke [128]. As many targets of WNT/β-Catenin were found to be unchanged in this study, further work is necessary to determine the mechanism and role of WNT/β-Catenin signaling in the alleviation of HFD-induced neuroinflammation and cognitive decline caused by FABP4 knockout. These studies will likely focus on isolated microglia from whole brain tissue. Single-cell RNA sequencing (scRNA-seq) has been used to define microglial immunoheterogeneity in models of AD [129,130]. Future studies using scRNA-seq to elucidate the microglial transcriptome changes that occur with FABP4 knockout in HFD-fed mice will provide further clarity on the mechanisms that lead to neuroprotection.

4. Materials and Methods

4.1. Mouse Model of Obesity and Immunometabolism

The FABP knockout mouse model (also known as aP2$^{-/-}$ or AKO mouse) carries a null mutation in FABP4 bred to wild-type C57BL/6J mouse background [16]. We refer to this transgenic mouse line (and tissue derived from these mice) as AKO mice. Genotyping was confirmed using PCR as previously described [16,124]. Mice were maintained in a 12:12 h light/dark cycle in a temperature-controlled room (21–22 °C) and were group-housed. WT and AKO mice ($n = 5$ per genotype) were placed on a high fat diet (HFD; Research Diets D12492; 60% total fat and 32% saturated fat) for 12 weeks starting at 15 weeks of age and water was provided ad libitum. The experimental protocol was approved by the Institutional Animal Care and Use Committee at the Minneapolis VAHCS.

4.2. Brain Dissection and RNA Isolation

Hippocampal tissue was rapidly dissected from WT and AKO mice sacrificed during the light phase, 5–8 h after lights on [131]. Total RNA was extracted from hippocampal tissue with the aid of Trizol (Invitrogen; Carlsbad, CA, USA), purified using the RNeasy Mini Kit (Qiagen, Hilden, Germany) and both procedures were performed according to the manufacturer's specification [131,132].

4.3. RNA-Seq cDNA Library Synthesis

Total RNA (3 μg) samples were sent to Novogene (Davis, CA, USA) for RNA-seq analysis. Briefly, RNA purity (OD260/OD280) was quantified using a Nanodrop spectrophotometer (Thermo Scientific; Waltham, MA, USA), RNA integrity and potential contamination was analyzed using agarose gel electrophoresis, and RNA integrity was

further analyzed using the Agilent 2100 bioanalyzer (Agilent Technologies, Santa Clara, CA, USA). mRNA was purified from total RNA using poly-T oligo-attached magnetic beads and mRNA was then fragmented randomly. All sequencing was performed in one batch. First strand cDNA was synthesized using random hexamer primer and M-MuLV Reverse Transcriptase Minus (RNase H−). Second strand cDNA synthesis was then performed using DNA Polymerase I and RNase H with dTTP replaced by dUTP. Double-stranded cDNA was purified using AMPure XP beads. Remaining overhangs of the purified double-stranded cDNA were converted into blunt ends via exonuclease/polymerase activities. After adenylation of 3′ ends of DNA fragments, NEBNext Adaptor with hairpin loop structure was ligated to prepare for hybridization. The second strand cDNA was then digested by USER enzyme. The final library was obtained by PCR amplification and purification of PCR products by AMPure XP beads. Library quality was ensured using the Agilent 2100 bioanalyzer (Agilent Technologies, Santa Clara, CA, USA). Clustering was performed on a cBot cluster generation system using the TruSeq PE Cluster Kit v3-cBot-HS (Illumina; San Diego, CA, USA). Library sequencing was performed using the Illumina HiSeq Platform (Illumina; San Diego, CA, USA).

4.4. RNA-Seq Analysis

Raw data (raw reads) were stored in FASTQ (fq) format. Raw reads containing adaptors, over 10% indeterminate bases, or over 50% low-quality bases were removed. Clean reads were mapped to a reference genome using STAR software. Differential expression analysis was performed using the DESeq2 R package. P-values were adjusted using Benjamini and Hochberg's procedure. Enrichment analysis of differentially expressed genes was performed using clusterProfiler software (version 3.16), including GO, DO, KEGG and Reactome database enrichment [133].

4.5. Reactome Analysis

Transcript quantification was performed with Salmon 1.0 [134] packaged in clusterProfiler 3.14.2 [135]. It was run with mapping mode selective alignment, minimum count of three, and relative abundance calculated in transcripts per million (TPM) relative to reference RNA transcripts from GENCODE VM23. Overrepresentation of transcripts and pathways and all other expression analysis was conducted with Reactome gene set analysis (ReactomeGSA) with Reactome pathway browser 3.7, database release 74 using the gene set enrichment analysis (GSEA) method and including disease pathways [136]. Within ReactomeGSA, normalization was performed with edgeR's calcNormFactors function, transformed using limma's voom and normalizeBetweenArrays functions, and pathway analysis using limma's camera function as implemented in the respective Bioconductor R package. Reactome identifiers are shown in square brackets and can be accessed at https://reactome.org. Unless otherwise noted, statistical significance was evaluated with a cutoff of ≤ 0.01 using the false discovery rate (FDR) as calculated using the Benjamini-Hochberg procedure for pathways and multiple correction adjusted *p*-values for transcripts (or genes). Transcript identifiers were translated to Ensembl gene IDs (names) with g:Profiler [137]. Additional ad hoc pathway analysis was conducted with GO, KEGG databases. Estimate surrogate cell type proportions variables were calculated with BRETIGEA [138]; input gene-level expression calculated by summing transcript TPMs per gene, and output with mouse species and separate runs with 20, 50, and 200 markers for all six cell types (astrocytes, endothelial cells, microglia, neurons, oligodendrocytes, and oligodendrocyte precursor cells). Senescence was evaluated with a list of 88 gene markers from the Tabula Muris Consortium [139].

4.6. Western Blotting

Western blotting was performed using dissected hippocampal tissues from AKO and WT mice as previously described. Tissue was homogenized in RIPA buffer (Thermo Scientific, Waltham, MA, USA) and PIC (HALT; Thermo Scientific, Waltham, MA, USA)

using a tissue homogenizer (Bullet Blender; Next Advance, Troy, NY, USA). Nuclear fractions were isolated using a nuclear extraction reagent (NE-PER; Thermo Scientific, Waltham, MA, USA). Protein concentration was determined using an infrared spectrometer (Direct Detect; Millipore, Burlington, MA, USA). 25 μg of protein was loaded onto a 4–20%, 30 μL-well precast gel (Bio-Rad, Hercules, CA, USA). Protein was transferred using the Trans-Blot Turbo system (Bio-Rad, Hercules, CA, USA). Total protein was stained using Licor Revert 700 stain (LI-COR, Lincoln, NE, USA) and imaged using the LI-COR Odyssey FC imager (LI-COR, Lincoln, NE, USA). Blocking was performed using Intercept Blocking Buffer (LI-COR, Lincoln, NE, USA). Primary antibody was used at 1:2000 dilution for a concentration of 1.25×10^{-1} μg/mL (BD Biosciences 610153; BD Biosciences, Franklin Lakes, NJ, USA), performed overnight at 4 °C with agitation. Secondary antibody was used at 1:10,000 dilution for a concentration of 1.0×10^{-1} μg/mL (LI-COR 926-32210; LI-COR, Lincoln, NE, USA) and imaged. Densitometry was performed using Image Studio software (LI-COR, Lincoln, NE, USA) and statistical analysis was performed using *t*-test (GraphPad Prism 7; GraphPad, San Diego, CA, USA).

References

1. Barnes, D.E.; Yaffe, K. The projected effect of risk factor reduction on Alzheimer's disease prevalence. *Lancet Neurol.* **2011**, *10*, 819–828. [CrossRef] [PubMed]
2. Miller, A.A.; Spencer, S.J. Obesity and neuroinflammation: A pathway to cognitive impairment. *Brain Behav. Immun.* **2014**, *42*, 10–21. [CrossRef] [PubMed]
3. Xu, W.L.; Atti, A.R.; Gatz, M.; Pedersen, N.L.; Johansson, B.; Fratiglioni, L. Midlife overweight and obesity increase late-life dementia risk: A population-based twin study. *Neurology* **2011**, *76*, 1568–1574. [CrossRef] [PubMed]

4. Cai, D. Neuroinflammation and neurodegeneration in overnutrition-induced diseases. *Trends Endocrinol. Metab.* **2013**, *24*, 40–47. [CrossRef] [PubMed]

5. Hotamisligil, G.S.; Shargill, N.S.; Spiegelman, B.M. Adipose expression of tumor necrosis factor-alpha: Direct role in obesity-linked insulin resistance. *Science* **1993**, *259*, 87–91. [CrossRef]

6. Thaler, J.P.; Yi, C.X.; Schur, E.A.; Guyenet, S.J.; Hwang, B.H.; Dietrich, M.O.; Zhao, X.; Sarruf, D.A.; Izgur, V.; Maravilla, K.R.; et al. Obesity is associated with hypothalamic injury in rodents and humans. *J. Clin. Investig.* **2012**, *122*, 153–162. [CrossRef]

7. Josephrajan, A.; Hertzel, A.V.; Bohm, E.K.; McBurney, M.W.; Imai, S.I.; Mashek, D.G.; Kim, D.H.; Bernlohr, D.A. Unconventional Secretion of Adipocyte Fatty Acid Binding Protein 4 Is Mediated By Autophagic Proteins in a Sirtuin-1-Dependent Manner. *Diabetes* **2019**, *68*, 1767–1777. [CrossRef]

8. Barrientos, R.M.; Kitt, M.M.; Watkins, L.R.; Maier, S.F. Neuroinflammation in the normal aging hippocampus. *Neuroscience* **2015**, *309*, 84–99. [CrossRef]

9. Ettcheto, M.; Petrov, D.; Pedros, I.; Alva, N.; Carbonell, T.; Beas-Zarate, C.; Pallas, M.; Auladell, C.; Folch, J.; Camins, A. Evaluation of Neuropathological Effects of a High-Fat Diet in a Presymptomatic Alzheimer's Disease Stage in APP/PS1 Mice. *J. Alzheimers Dis.* **2016**, *54*, 233–251. [CrossRef]

10. Hao, S.; Dey, A.; Yu, X.; Stranahan, A.M. Dietary obesity reversibly induces synaptic stripping by microglia and impairs hippocampal plasticity. *Brain Behav. Immun.* **2016**, *51*, 230–239. [CrossRef]

11. Karmi, A.; Iozzo, P.; Viljanen, A.; Hirvonen, J.; Fielding, B.A.; Virtanen, K.; Oikonen, V.; Kemppainen, J.; Viljanen, T.; Guiducci, L.; et al. Increased brain fatty acid uptake in metabolic syndrome. *Diabetes* **2010**, *59*, 2171–2177. [CrossRef]

12. Nam, K.N.; Mounier, A.; Wolfe, C.M.; Fitz, N.F.; Carter, A.Y.; Castranio, E.L.; Kamboh, H.I.; Reeves, V.L.; Wang, J.; Han, X.; et al. Effect of high fat diet on phenotype, brain transcriptome and lipidome in Alzheimer's model mice. *Sci. Rep.* **2017**, *7*, 4307. [CrossRef]

13. Pistell, P.J.; Morrison, C.D.; Gupta, S.; Knight, A.G.; Keller, J.N.; Ingram, D.K.; Bruce-Keller, A.J. Cognitive impairment following high fat diet consumption is associated with brain inflammation. *J. Neuroimmunol.* **2010**, *219*, 25–32. [CrossRef]

14. Valdearcos, M.; Douglass, J.D.; Robblee, M.M.; Dorfman, M.D.; Stifler, D.R.; Bennett, M.L.; Gerritse, I.; Fasnacht, R.; Barres, B.A.; Thaler, J.P.; et al. Microglial Inflammatory Signaling Orchestrates the Hypothalamic Immune Response to Dietary Excess and Mediates Obesity Susceptibility. *Cell Metab.* **2017**, *26*, 185–197.e183. [CrossRef]

15. Valdearcos, M.; Robblee, M.M.; Benjamin, D.I.; Nomura, D.K.; Xu, A.W.; Koliwad, S.K. Microglia dictate the impact of saturated fat consumption on hypothalamic inflammation and neuronal function. *Cell Rep.* **2014**, *9*, 2124–2138. [CrossRef]

16. Hotamisligil, G.S.; Johnson, R.S.; Distel, R.J.; Ellis, R.; Papaioannou, V.E.; Spiegelman, B.M. Uncoupling of obesity from insulin resistance through a targeted mutation in aP2, the adipocyte fatty acid binding protein. *Science* **1996**, *274*, 1377–1379. [CrossRef]

17. Shum, B.O.; Mackay, C.R.; Gorgun, C.Z.; Frost, M.J.; Kumar, R.K.; Hotamisligil, G.S.; Rolph, M.S. The adipocyte fatty acid-binding protein aP2 is required in allergic airway inflammation. *J. Clin. Investig.* **2006**, *116*, 2183–2192. [CrossRef]

18. Furuhashi, M.; Tuncman, G.; Gorgun, C.Z.; Makowski, L.; Atsumi, G.; Vaillancourt, E.; Kono, K.; Babaev, V.R.; Fazio, S.; Linton, M.F.; et al. Treatment of diabetes and atherosclerosis by inhibiting fatty-acid-binding protein aP2. *Nature* **2007**, *447*, 959–965. [CrossRef]

19. Boord, J.B.; Maeda, K.; Makowski, L.; Babaev, V.R.; Fazio, S.; Linton, M.F.; Hotamisligil, G.S. Combined adipocyte-macrophage fatty acid-binding protein deficiency improves metabolism, atherosclerosis, and survival in apolipoprotein E-deficient mice. *Circulation* **2004**, *110*, 1492–1498. [CrossRef]

20. Xu, H.; Hertzel, A.V.; Steen, K.A.; Wang, Q.; Suttles, J.; Bernlohr, D.A. Uncoupling lipid metabolism from inflammation through fatty acid binding protein-dependent expression of UCP2. *Mol. Cell. Biol.* **2015**, *35*, 1055–1065. [CrossRef]

21. Hotamisligil, G.S.; Bernlohr, D.A. Metabolic functions of FABPs—Mechanisms and therapeutic implications. *Nat. Rev. Endocrinol.* **2015**, *11*, 592–605. [CrossRef] [PubMed]

22. Hotamisligil, G.S. Inflammation, metaflammation and immunometabolic disorders. *Nature* **2017**, *542*, 177–185. [CrossRef] [PubMed]

23. So, S.W.; Fleming, K.M.; Duffy, C.M.; Nixon, J.P.; Bernlohr, D.A.; Butterick, T.A. Microglial FABP4-UCP2 Axis Modulates Neuroinflammation and Cognitive Decline in Obese Mice. *Int. J. Mol. Sci.* **2022**, *23*, 4354. [CrossRef] [PubMed]

24. Duffy, C.M.; Xu, H.; Nixon, J.P.; Bernlohr, D.A.; Butterick, T.A. Identification of a fatty acid binding protein4-UCP2 axis regulating microglial mediated neuroinflammation. *Mol. Cell. Neurosci.* **2017**, *80*, 52–57. [CrossRef]

25. Leow, S.C.; Poschmann, J.; Too, P.G.; Yin, J.; Joseph, R.; McFarlane, C.; Dogra, S.; Shabbir, A.; Ingham, P.W.; Prabhakar, S.; et al. The transcription factor SOX6 contributes to the developmental origins of obesity by promoting adipogenesis. *Development* **2016**, *143*, 950–961. [CrossRef]

26. Fath, T.; Fischer, R.S.; Dehmelt, L.; Halpain, S.; Fowler, V.M. Tropomodulins are negative regulators of neurite outgrowth. *Eur. J. Cell Biol.* **2011**, *90*, 291–300. [CrossRef]

27. Ma, C.; Li, J.; Bao, Z.; Ruan, Q.; Yu, Z. Serum Levels of ApoA1 and ApoA2 Are Associated with Cognitive Status in Older Men. *Biomed. Res. Int.* **2015**, *2015*, 481621. [CrossRef]

28. Gu, X.; Yao, X.; Liu, D. Up-regulation of microRNA-335-5p reduces inflammation via negative regulation of the TPX2-mediated AKT/GSK3β signaling pathway in a chronic rhinosinusitis mouse model. *Cell. Signal.* **2020**, *70*, 109596. [CrossRef]

29. Shami, A.; Knutsson, A.; Duner, P.; Rauch, U.; Bengtsson, E.; Tengryd, C.; Murugesan, V.; Durbeej, M.; Goncalves, I.; Nilsson, J.; et al. Dystrophin deficiency reduces atherosclerotic plaque development in ApoE-null mice. *Sci. Rep.* **2015**, *5*, 13904. [CrossRef]

30. Singh, B.K.; Vatsa, N.; Kumar, V.; Shekhar, S.; Sharma, A.; Jana, N.R. Ube3a deficiency inhibits amyloid plaque formation in APPswe/PS1deltaE9 mouse model of Alzheimer's disease. *Hum. Mol. Genet.* **2017**, *26*, 4042–4054. [CrossRef]

31. Hori, O.; Ichinoda, F.; Tamatani, T.; Yamaguchi, A.; Sato, N.; Ozawa, K.; Kitao, Y.; Miyazaki, M.; Harding, H.P.; Ron, D.; et al. Transmission of cell stress from endoplasmic reticulum to mitochondria: Enhanced expression of Lon protease. *J. Cell Biol.* **2002**, *157*, 1151–1160. [CrossRef]

32. Yang, M.; Liu, Y.; Dai, J.; Li, L.; Ding, X.; Xu, Z.; Mori, M.; Miyahara, H.; Sawashita, J.; Higuchi, K. Apolipoprotein A-II induces acute-phase response associated AA amyloidosis in mice through conformational changes of plasma lipoprotein structure. *Sci. Rep.* **2018**, *8*, 5620. [CrossRef]

33. Berrios, J.; Stamatakis, A.M.; Kantak, P.A.; McElligott, Z.A.; Judson, M.C.; Aita, M.; Rougie, M.; Stuber, G.D.; Philpot, B.D. Loss of UBE3A from TH-expressing neurons suppresses GABA co-release and enhances VTA-NAc optical self-stimulation. *Nat. Commun.* **2016**, *7*, 10702. [CrossRef]

34. Sun, Y.; Shestakova, A.; Hunt, L.; Sehgal, S.; Lupashin, V.; Storrie, B. Rab6 regulates both ZW10/RINT-1 and conserved oligomeric Golgi complex-dependent Golgi trafficking and homeostasis. *Mol. Biol. Cell* **2007**, *18*, 4129–4142. [CrossRef]

35. Vaillend, C.; Chaussenot, R. Relationships linking emotional, motor, cognitive and GABAergic dysfunctions in dystrophin-deficient mdx mice. *Hum. Mol. Genet.* **2017**, *26*, 1041–1055. [CrossRef]

36. Li, X.; An, W.L.; Alafuzoff, I.; Soininen, H.; Winblad, B.; Pei, J.J. Phosphorylated eukaryotic translation factor 4E is elevated in Alzheimer brain. *Neuroreport* **2004**, *15*, 2237–2240. [CrossRef]

37. Smith, J.R.; Hayman, G.T.; Wang, S.J.; Laulederkind, S.J.F.; Hoffman, M.J.; Kaldunski, M.L.; Tutaj, M.; Thota, J.; Nalabolu, H.S.; Ellanki, S.L.R.; et al. The Year of the Rat: The Rat Genome Database at 20: A multi-species knowledgebase and analysis platform. *Nucleic Acids Res.* **2020**, *48*, D731–D742. [CrossRef]

38. York, W.S.; Mazumder, R.; Ranzinger, R.; Edwards, N.; Kahsay, R.; Aoki-Kinoshita, K.F.; Campbell, M.P.; Cummings, R.D.; Feizi, T.; Martin, M.; et al. GlyGen: Computational and Informatics Resources for Glycoscience. *Glycobiology* **2020**, *30*, 72–73. [CrossRef]

39. Lupo, A.; Cesaro, E.; Montano, G.; Zurlo, D.; Izzo, P.; Costanzo, P. KRAB-Zinc Finger Proteins: A Repressor Family Displaying Multiple Biological Functions. *Curr. Genomics* **2013**, *14*, 268–278. [CrossRef]

40. Ping, X.L.; Sun, B.F.; Wang, L.; Xiao, W.; Yang, X.; Wang, W.J.; Adhikari, S.; Shi, Y.; Lv, Y.; Chen, Y.S.; et al. Mammalian WTAP is a regulatory subunit of the RNA N6-methyladenosine methyltransferase. *Cell Res.* **2014**, *24*, 177–189. [CrossRef]

41. Han, M.; Liu, Z.; Xu, Y.; Liu, X.; Wang, D.; Li, F.; Wang, Y.; Bi, J. Abnormality of m6A mRNA Methylation Is Involved in Alzheimer's Disease. *Front. Neurosci.* **2020**, *14*, 98. [CrossRef] [PubMed]

42. Wang, M.; Wey, S.; Zhang, Y.; Ye, R.; Lee, A.S. Role of the unfolded protein response regulator GRP78/BiP in development, cancer, and neurological disorders. *Antioxid. Redox Signal.* **2009**, *11*, 2307–2316. [CrossRef] [PubMed]

43. Magini, P.; Smits, D.J.; Vandervore, L.; Schot, R.; Columbaro, M.; Kasteleijn, E.; van der Ent, M.; Palombo, F.; Lequin, M.H.; Dremmen, M.; et al. Loss of SMPD4 Causes a Developmental Disorder Characterized by Microcephaly and Congenital Arthrogryposis. *Am. J. Hum. Genet.* **2019**, *105*, 689–705. [CrossRef] [PubMed]

44. Dong, S.S.; Zhu, D.L.; Zhou, X.R.; Rong, Y.; Zeng, M.; Chen, J.B.; Jiang, F.; Tuo, X.M.; Feng, Z.; Yang, T.L.; et al. An Intronic Risk SNP rs12454712 for Central Obesity Acts As an Allele-Specific Enhancer To Regulate BCL2 Expression. *Diabetes* **2021**, *70*, 1679–1688. [CrossRef] [PubMed]

45. Corbett, B.F.; Luz, S.; Arner, J.; Pearson-Leary, J.; Sengupta, A.; Taylor, D.; Gehrman, P.; Ross, R.; Bhatnagar, S. Sphingosine-1-phosphate receptor 3 in the medial prefrontal cortex promotes stress resilience by reducing inflammatory processes. *Nat. Commun.* **2019**, *10*, 3146. [CrossRef]

46. Huang, G.Z.; Taniguchi, M.; Zhou, Y.B.; Zhang, J.J.; Okutani, F.; Murata, Y.; Yamaguchi, M.; Kaba, H. α2-Adrenergic receptor activation promotes long-term potentiation at excitatory synapses in the mouse accessory olfactory bulb. *Learn Mem.* **2018**, *25*, 147–157. [CrossRef]

47. Connor, S.A.; Ammendrup-Johnsen, I.; Kishimoto, Y.; Karimi Tari, P.; Cvetkovska, V.; Harada, T.; Ojima, D.; Yamamoto, T.; Wang, Y.T.; Craig, A.M. Loss of Synapse Repressor MDGA1 Enhances Perisomatic Inhibition, Confers Resistance to Network Excitation, and Impairs Cognitive Function. *Cell Rep.* **2017**, *21*, 3637–3645. [CrossRef]

48. Petrovic, M.M.; Viana da Silva, S.; Clement, J.P.; Vyklicky, L.; Mulle, C.; Gonzalez-Gonzalez, I.M.; Henley, J.M. Metabotropic action of postsynaptic kainate receptors triggers hippocampal long-term potentiation. *Nat. Neurosci.* **2017**, *20*, 529–539. [CrossRef]

49. Weth-Malsch, D.; Langeslag, M.; Beroukas, D.; Zangrandi, L.; Kastenberger, I.; Quarta, S.; Malsch, P.; Kalpachidou, T.; Schwarzer, C.; Proia, R.L.; et al. Ablation of Sphingosine 1-Phosphate Receptor Subtype 3 Impairs Hippocampal Neuron Excitability In vitro and Spatial Working Memory In vivo. *Front. Cell. Neurosci.* **2016**, *10*, 258. [CrossRef]

50. Singh, P.; Konar, A.; Kumar, A.; Srivas, S.; Thakur, M.K. Hippocampal chromatin-modifying enzymes are pivotal for scopolamine-induced synaptic plasticity gene expression changes and memory impairment. *J. Neurochem.* **2015**, *134*, 642–651. [CrossRef]

51. Rasmussen, A.H.; Rasmussen, H.B.; Silahtaroglu, A. The DLGAP family: Neuronal expression, function and role in brain disorders. *Mol. Brain* **2017**, *10*, 43. [CrossRef]

52. Schneider, J.W.; Goetsch, S.C.; Leng, X.; Ludwig, S.M.; Russell, J.L.; Yang, C.P.; Zhang, Q.J. Coupling hippocampal neurogenesis to brain pH through proneurogenic small molecules that regulate proton sensing G protein-coupled receptors. *ACS Chem. Neurosci.* **2012**, *3*, 557–568. [CrossRef]

53. Noguchi, H.; Castillo, J.G.; Nakashima, K.; Pleasure, S.J. Suppressor of fused controls perinatal expansion and quiescence of future dentate adult neural stem cells. *Elife* **2019**, *8*, e42918. [CrossRef]

54. Kajla, S.; Mondol, A.S.; Nagasawa, A.; Zhang, Y.; Kato, M.; Matsuno, K.; Yabe-Nishimura, C.; Kamata, T. A crucial role for Nox 1 in redox-dependent regulation of Wnt-β-catenin signaling. *FASEB J.* **2012**, *26*, 2049–2059. [CrossRef]

55. Asaro, A.; Carlo-Spiewok, A.S.; Malik, A.R.; Rothe, M.; Schipke, C.G.; Peters, O.; Heeren, J.; Willnow, T.E. Apolipoprotein E4 disrupts the neuroprotective action of sortilin in neuronal lipid metabolism and endocannabinoid signaling. *Alzheimers Dement.* **2020**, *16*, 1248–1258. [CrossRef]

56. Carlo, A.S.; Gustafsen, C.; Mastrobuoni, G.; Nielsen, M.S.; Burgert, T.; Hartl, D.; Rohe, M.; Nykjaer, A.; Herz, J.; Heeren, J.; et al. The pro-neurotrophin receptor sortilin is a major neuronal apolipoprotein E receptor for catabolism of amyloid-β peptide in the brain. *J. Neurosci.* **2013**, *33*, 358–370. [CrossRef]

57. Goldberg, J.; Currais, A.; Ates, G.; Huang, L.; Shokhirev, M.; Maher, P.; Schubert, D. Targeting of intracellular Ca^{2+} stores as a therapeutic strategy against age-related neurotoxicities. *NPJ Aging Mech. Dis.* **2020**, *6*, 10. [CrossRef]

58. Kong, W.; Mou, X.; Zhang, N.; Zeng, W.; Li, S.; Yang, Y. The construction of common and specific significance subnetworks of Alzheimer's disease from multiple brain regions. *Biomed Res. Int.* **2015**, *2015*, 394260. [CrossRef]

59. Gangwar, S.P.; Zhong, X.; Seshadrinathan, S.; Chen, H.; Machius, M.; Rudenko, G. Molecular Mechanism of MDGA1: Regulation of Neuroligin 2:Neurexin Trans-synaptic Bridges. *Neuron* **2017**, *94*, 1132–1141.e1134. [CrossRef]

60. UniProt, C. UniProt: The universal protein knowledgebase in 2021. *Nucleic Acids Res.* **2021**, *49*, D480–D489. [CrossRef]

61. Xu, D.; Wang, Z.; Zhang, Y.; Jiang, W.; Pan, Y.; Song, B.L.; Chen, Y. PAQR3 modulates cholesterol homeostasis by anchoring Scap/SREBP complex to the Golgi apparatus. *Nat. Commun.* **2015**, *6*, 8100. [CrossRef] [PubMed]

62. Deng, S.; Liu, J.; Wu, X.; Lu, W. Golgi Apparatus: A Potential Therapeutic Target for Autophagy-Associated Neurological Diseases. *Front. Cell Dev. Biol.* **2020**, *8*, 564975. [CrossRef] [PubMed]

63. Christensen, J.H.; Elfving, B.; Muller, H.K.; Fryland, T.; Nyegaard, M.; Corydon, T.J.; Nielsen, A.L.; Mors, O.; Wegener, G.; Borglum, A.D. The Schizophrenia and Bipolar Disorder associated BRD1 gene is regulated upon chronic restraint stress. *Eur. Neuropsychopharmacol.* **2012**, *22*, 651–656. [CrossRef] [PubMed]

64. Ireland, D.R.; Abraham, W.C. Group I mGluRs increase excitability of hippocampal CA1 pyramidal neurons by a PLC-independent mechanism. *J. Neurophysiol.* **2002**, *88*, 107–116. [CrossRef]

65. Hwang, J.Y.; Aromolaran, K.A.; Zukin, R.S. The emerging field of epigenetics in neurodegeneration and neuroprotection. *Nat. Rev. Neurosci.* **2017**, *18*, 347–361. [CrossRef]

66. Ko, Y.U.; Kim, C.; Lee, J.; Kim, D.; Kim, Y.; Yun, N.; Oh, Y.J. Site-specific phosphorylation of Fbxw7 by Cdk5/p25 and its resulting decreased stability are linked to glutamate-induced excitotoxicity. *Cell Death Dis.* **2019**, *10*, 579. [CrossRef]

67. Xu, Q.; Choksi, S.; Qu, J.; Jang, J.; Choe, M.; Banfi, B.; Engelhardt, J.F.; Liu, Z.G. NADPH Oxidases Are Essential for Macrophage Differentiation. *J. Biol. Chem.* **2016**, *291*, 20030–20041. [CrossRef]

68. Stojakovic, A.; Trushin, S.; Sheu, A.; Khalili, L.; Chang, S.Y.; Li, X.; Christensen, T.; Salisbury, J.L.; Geroux, R.E.; Gateno, B.; et al. Partial inhibition of mitochondrial complex I ameliorates Alzheimer's disease pathology and cognition in APP/PS1 female mice. *Commun. Biol.* **2021**, *4*, 61. [CrossRef]

69. Schiff, M.; Haberberger, B.; Xia, C.; Mohsen, A.W.; Goetzman, E.S.; Wang, Y.; Uppala, R.; Zhang, Y.; Karunanidhi, A.; Prabhu, D.; et al. Complex I assembly function and fatty acid oxidation enzyme activity of ACAD9 both contribute to disease severity in ACAD9 deficiency. *Hum. Mol. Genet.* **2015**, *24*, 3238–3247. [CrossRef]

70. Kumar, R.; Corbett, M.A.; Smith, N.J.C.; Hock, D.H.; Kikhtyak, Z.; Semcesen, L.N.; Morimoto, A.; Lee, S.; Stroud, D.A.; Gleeson, J.G.; et al. Oligonucleotide correction of an intronic TIMMDC1 variant in cells of patients with severe neurodegenerative disorder. *NPJ Genom. Med.* **2022**, *7*, 9. [CrossRef]

71. Fukui, H.; Diaz, F.; Garcia, S.; Moraes, C.T. Cytochrome c oxidase deficiency in neurons decreases both oxidative stress and amyloid formation in a mouse model of Alzheimer's disease. *Proc. Natl. Acad. Sci. USA* **2007**, *104*, 14163–14168. [CrossRef]

72. Okazaki, M.; Ishibashi, Y.; Asoh, S.; Ohta, S. Overexpressed mitochondrial hinge protein, a cytochrome c-binding protein, accelerates apoptosis by enhancing the release of cytochrome c from mitochondria. *Biochem. Biophys. Res. Commun.* **1998**, *243*, 131–136. [CrossRef]

73. Kim, S.H.; Vlkolinsky, R.; Cairns, N.; Lubec, G. Decreased levels of complex III core protein 1 and complex V beta chain in brains from patients with Alzheimer's disease and Down syndrome. *Cell. Mol. Life Sci.* **2000**, *57*, 1810–1816. [CrossRef]

74. Pomytkin, I.; Pinelis, V. Brain Insulin Resistance: Focus on Insulin Receptor-Mitochondria Interactions. *Life* **2021**, *11*, 262. [CrossRef]

75. Richman, T.R.; Spahr, H.; Ermer, J.A.; Davies, S.M.; Viola, H.M.; Bates, K.A.; Papadimitriou, J.; Hool, L.C.; Rodger, J.; Larsson, N.G.; et al. Loss of the RNA-binding protein TACO1 causes late-onset mitochondrial dysfunction in mice. *Nat. Commun.* **2016**, *7*, 11884. [CrossRef]

76. Mangialasche, F.; Baglioni, M.; Cecchetti, R.; Kivipelto, M.; Ruggiero, C.; Piobbico, D.; Kussmaul, L.; Monastero, R.; Brancorsini, S.; Mecocci, P. Lymphocytic mitochondrial aconitase activity is reduced in Alzheimer's disease and mild cognitive impairment. *J. Alzheimers Dis.* **2015**, *44*, 649–660. [CrossRef]

77. Seim, G.L.; Britt, E.C.; John, S.V.; Yeo, F.J.; Johnson, A.R.; Eisenstein, R.S.; Pagliarini, D.J.; Fan, J. Two-stage metabolic remodelling in macrophages in response to lipopolysaccharide and interferon-gamma stimulation. *Nat. Metab.* **2019**, *1*, 731–742. [CrossRef]

78. Fisar, Z.; Hroudova, J.; Hansikova, H.; Spacilova, J.; Lelkova, P.; Wenchich, L.; Jirak, R.; Zverova, M.; Zeman, J.; Martasek, P.; et al. Mitochondrial Respiration in the Platelets of Patients with Alzheimer's Disease. *Curr. Alzheimer Res.* **2016**, *13*, 930–941. [CrossRef]

79. Nakai, N.; Obayashi, M.; Nagasaki, M.; Sato, Y.; Fujitsuka, N.; Yoshimura, A.; Miyazaki, Y.; Sugiyama, S.; Shimomura, Y. The abundance of mRNAs for pyruvate dehydrogenase kinase isoenzymes in brain regions of young and aged rats. *Life Sci.* **2000**, *68*, 497–503. [CrossRef]

80. Bos, C.L.; Kodach, L.L.; van den Brink, G.R.; Diks, S.H.; van Santen, M.M.; Richel, D.J.; Peppelenbosch, M.P.; Hardwick, J.C. Effect of aspirin on the Wnt/β-catenin pathway is mediated via protein phosphatase 2A. *Oncogene* **2006**, *25*, 6447–6456. [CrossRef]

81. Sun, L.; Liu, S.Y.; Zhou, X.W.; Wang, X.C.; Liu, R.; Wang, Q.; Wang, J.Z. Inhibition of protein phosphatase 2A- and protein phosphatase 1-induced tau hyperphosphorylation and impairment of spatial memory retention in rats. *Neuroscience* **2003**, *118*, 1175–1182. [CrossRef] [PubMed]

82. Guo, X.; Waddell, D.S.; Wang, W.; Wang, Z.; Liberati, N.T.; Yong, S.; Liu, X.; Wang, X.F. Ligand-dependent ubiquitination of Smad3 is regulated by casein kinase 1 gamma 2, an inhibitor of TGF-β signaling. *Oncogene* **2008**, *27*, 7235–7247. [CrossRef] [PubMed]

83. Jia, L.; Pina-Crespo, J.; Li, Y. Restoring Wnt/β-catenin signaling is a promising therapeutic strategy for Alzheimer's disease. *Mol. Brain* **2019**, *12*, 104. [CrossRef] [PubMed]

84. Wang, M.; Liu, X.; Hou, Y.; Zhang, H.; Kang, J.; Wang, F.; Zhao, Y.; Chen, J.; Liu, X.; Wang, Y.; et al. Decrease of GSK-3β Activity in the Anterior Cingulate Cortex of Shank3b (-/-) Mice Contributes to Synaptic and Social Deficiency. *Front. Cell. Neurosci.* **2019**, *13*, 447. [CrossRef] [PubMed]

85. Mardones, M.D.; Andaur, G.A.; Varas-Godoy, M.; Henriquez, J.F.; Salech, F.; Behrens, M.I.; Couve, A.; Inestrosa, N.C.; Varela-Nallar, L. Frizzled-1 receptor regulates adult hippocampal neurogenesis. *Mol. Brain* **2016**, *9*, 29. [CrossRef]

86. Goldberg, J.; Currais, A.; Prior, M.; Fischer, W.; Chiruta, C.; Ratliff, E.; Daugherty, D.; Dargusch, R.; Finley, K.; Esparza-Molto, P.B.; et al. The mitochondrial ATP synthase is a shared drug target for aging and dementia. *Aging Cell* **2018**, *17*. [CrossRef]

87. Martinez, F.O.; Gordon, S.; Locati, M.; Mantovani, A. Transcriptional profiling of the human monocyte-to-macrophage differentiation and polarization: New molecules and patterns of gene expression. *J. Immunol.* **2006**, *177*, 7303–7311. [CrossRef]

88. Ogasawara, M.; Kim, S.C.; Adamik, R.; Togawa, A.; Ferrans, V.J.; Takeda, K.; Kirby, M.; Moss, J.; Vaughan, M. Similarities in function and gene structure of cytohesin-4 and cytohesin-1, guanine nucleotide-exchange proteins for ADP-ribosylation factors. *J. Biol. Chem.* **2000**, *275*, 3221–3230. [CrossRef]

89. Robinson, D.G.; Scheuring, D.; Naramoto, S.; Friml, J. ARF1 localizes to the golgi and the trans-golgi network. *Plant Cell* **2011**, *23*, 846–849. [CrossRef]

90. Choi, D.Y.; Lee, M.K.; Hong, J.T. Lack of CCR5 modifies glial phenotypes and population of the nigral dopaminergic neurons, but not MPTP-induced dopaminergic neurodegeneration. *Neurobiol. Dis.* **2013**, *49*, 159–168. [CrossRef]

91. Bonilla, F.A.; Fujita, R.M.; Pivniouk, V.I.; Chan, A.C.; Geha, R.S. Adapter proteins SLP-76 and BLNK both are expressed by murine macrophages and are linked to signaling via Fcγ receptors I and II/III. *Proc. Natl. Acad. Sci. USA* **2000**, *97*, 1725–1730. [CrossRef]

92. Rogers, J.T.; Morganti, J.M.; Bachstetter, A.D.; Hudson, C.E.; Peters, M.M.; Grimmig, B.A.; Weeber, E.J.; Bickford, P.C.; Gemma, C. CX3CR1 deficiency leads to impairment of hippocampal cognitive function and synaptic plasticity. *J. Neurosci.* **2011**, *31*, 16241–16250. [CrossRef]

93. Schaeffer, E.L.; Gattaz, W.F. Requirement of hippocampal phospholipase A2 activity for long-term memory retrieval in rats. *J. Neural Transm.* **2007**, *114*, 379–385. [CrossRef]

94. Palla, A.R.; Ravichandran, M.; Wang, Y.X.; Alexandrova, L.; Yang, A.V.; Kraft, P.; Holbrook, C.A.; Schurch, C.M.; Ho, A.T.V.; Blau, H.M. Inhibition of prostaglandin-degrading enzyme 15-PGDH rejuvenates aged muscle mass and strength. *Science* **2021**, *371*, eabc8059. [CrossRef]

95. Kawamura, N.; Katsuura, G.; Yamada-Goto, N.; Novianti, E.; Inui, A.; Asakawa, A. Impaired brain fractalkine-CX3CR1 signaling is implicated in cognitive dysfunction in diet-induced obese mice. *BMJ Open Diabetes Res. Care* **2021**, *9*, e001492. [CrossRef]

96. Barros, M.H.; Hauck, F.; Dreyer, J.H.; Kempkes, B.; Niedobitek, G. Macrophage polarisation: An immunohistochemical approach for identifying M1 and M2 macrophages. *PLoS ONE* **2013**, *8*, e80908. [CrossRef]

97. Park, M.H.; Lee, Y.K.; Lee, Y.H.; Kim, Y.B.; Yun, Y.W.; Nam, S.Y.; Hwang, S.J.; Han, S.B.; Kim, S.U.; Hong, J.T. Chemokines released from astrocytes promote chemokine receptor 5-mediated neuronal cell differentiation. *Exp. Cell Res.* **2009**, *315*, 2715–2726. [CrossRef]

98. Rangaraju, S.; Dammer, E.B.; Raza, S.A.; Rathakrishnan, P.; Xiao, H.; Gao, T.; Duong, D.M.; Pennington, M.W.; Lah, J.J.; Seyfried, N.T.; et al. Identification and therapeutic modulation of a pro-inflammatory subset of disease-associated-microglia in Alzheimer's disease. *Mol. Neurodegener.* **2018**, *13*, 24. [CrossRef]

99. Uranga, R.M.; Bruce-Keller, A.J.; Morrison, C.D.; Fernandez-Kim, S.O.; Ebenezer, P.J.; Zhang, L.; Dasuri, K.; Keller, J.N. Intersection between metabolic dysfunction, high fat diet consumption, and brain aging. *J. Neurochem.* **2010**, *114*, 344–361. [CrossRef]

100. Duan, Y.; Zeng, L.; Zheng, C.; Song, B.; Li, F.; Kong, X.; Xu, K. Inflammatory Links Between High Fat Diets and Diseases. *Front. Immunol.* **2018**, *9*, 2649. [CrossRef]

101. Melo, H.M.; Santos, L.E.; Ferreira, S.T. Diet-Derived Fatty Acids, Brain Inflammation, and Mental Health. *Front. Neurosci.* **2019**, *13*, 265. [CrossRef] [PubMed]

102. O'Brien, P.D.; Hinder, L.M.; Callaghan, B.C.; Feldman, E.L. Neurological consequences of obesity. *Lancet Neurol.* **2017**, *16*, 465–477. [CrossRef] [PubMed]

103. Milanski, M.; Degasperi, G.; Coope, A.; Morari, J.; Denis, R.; Cintra, D.E.; Tsukumo, D.M.; Anhe, G.; Amaral, M.E.; Takahashi, H.K.; et al. Saturated fatty acids produce an inflammatory response predominantly through the activation of TLR4 signaling in hypothalamus: Implications for the pathogenesis of obesity. *J. Neurosci.* **2009**, *29*, 359–370. [CrossRef] [PubMed]

104. Jepson, J.E.C.; Praschberger, R.; Krishnakumar, S.S. Mechanisms of Neurological Dysfunction in GOSR2 Progressive Myoclonus Epilepsy, a Golgi SNAREopathy. *Neuroscience* **2019**, *420*, 41–49. [CrossRef] [PubMed]

105. Sapperstein, S.K.; Walter, D.M.; Grosvenor, A.R.; Heuser, J.E.; Waters, M.G. p115 is a general vesicular transport factor related to the yeast endoplasmic reticulum to Golgi transport factor Uso1p. *Proc. Natl. Acad. Sci. USA* **1995**, *92*, 522–526. [CrossRef]

106. Izumi, K.; Brett, M.; Nishi, E.; Drunat, S.; Tan, E.S.; Fujiki, K.; Lebon, S.; Cham, B.; Masuda, K.; Arakawa, M.; et al. ARCN1 Mutations Cause a Recognizable Craniofacial Syndrome Due to COPI-Mediated Transport Defects. *Am. J. Hum. Genet.* **2016**, *99*, 451–459. [CrossRef]

107. LaMonte, B.H.; Wallace, K.E.; Holloway, B.A.; Shelly, S.S.; Ascano, J.; Tokito, M.; Van Winkle, T.; Howland, D.S.; Holzbaur, E.L. Disruption of dynein/dynactin inhibits axonal transport in motor neurons causing late-onset progressive degeneration. *Neuron* **2002**, *34*, 715–727. [CrossRef]

108. Mkhikian, H.; Grigorian, A.; Li, C.F.; Chen, H.L.; Newton, B.; Zhou, R.W.; Beeton, C.; Torossian, S.; Tatarian, G.G.; Lee, S.U.; et al. Genetics and the environment converge to dysregulate *N*-glycosylation in multiple sclerosis. *Nat. Commun.* **2011**, *2*, 334. [CrossRef]

109. Bankaitis, V.A.; Garcia-Mata, R.; Mousley, C.J. Golgi membrane dynamics and lipid metabolism. *Curr. Biol.* **2012**, *22*, R414–R424. [CrossRef]

110. Zaki, M.E.; Amr, K.S.; Abdel-Hamid, M. APOA2 Polymorphism in Relation to Obesity and Lipid Metabolism. *Cholesterol* **2013**, *2013*, 289481. [CrossRef]

111. Su, X.; Chen, L.; Chen, X.; Dai, C.; Wang, B. Emerging roles of sortilin in affecting the metabolism of glucose and lipid profiles. *Bosn. J. Basic Med. Sci.* **2022**, *22*, 340–352. [CrossRef]

112. Nakandakari, S.; Munoz, V.R.; Kuga, G.K.; Gaspar, R.C.; Sant'Ana, M.R.; Pavan, I.C.B.; da Silva, L.G.S.; Morelli, A.P.; Simabuco, F.M.; da Silva, A.S.R.; et al. Short-term high-fat diet modulates several inflammatory, ER stress, and apoptosis markers in the hippocampus of young mice. *Brain Behav. Immun.* **2019**, *79*, 284–293. [CrossRef]

113. Uddin, M.S.; Yu, W.S.; Lim, L.W. Exploring ER stress response in cellular aging and neuroinflammation in Alzheimer's disease. *Ageing Res. Rev.* **2021**, *70*, 101417. [CrossRef]

114. Su, J.H.; Zhao, M.; Anderson, A.J.; Srinivasan, A.; Cotman, C.W. Activated caspase-3 expression in Alzheimer's and aged control brain: Correlation with Alzheimer pathology. *Brain Res.* **2001**, *898*, 350–357. [CrossRef]

115. Hollands, C.; Tobin, M.K.; Hsu, M.; Musaraca, K.; Yu, T.S.; Mishra, R.; Kernie, S.G.; Lazarov, O. Depletion of adult neurogenesis exacerbates cognitive deficits in Alzheimer's disease by compromising hippocampal inhibition. *Mol. Neurodegener.* **2017**, *12*, 64. [CrossRef]

116. Boric, K.; Munoz, P.; Gallagher, M.; Kirkwood, A. Potential adaptive function for altered long-term potentiation mechanisms in aging hippocampus. *J. Neurosci.* **2008**, *28*, 8034–8039. [CrossRef]

117. Arredondo, S.B.; Valenzuela-Bezanilla, D.; Mardones, M.D.; Varela-Nallar, L. Role of Wnt Signaling in Adult Hippocampal Neurogenesis in Health and Disease. *Front. Cell Dev. Biol.* **2020**, *8*, 860. [CrossRef]

118. Tapia-Rojas, C.; Inestrosa, N.C. Loss of canonical Wnt signaling is involved in the pathogenesis of Alzheimer's disease. *Neural Regen. Res.* **2018**, *13*, 1705–1710. [CrossRef]

119. De Ferrari, G.V.; Avila, M.E.; Medina, M.A.; Perez-Palma, E.; Bustos, B.I.; Alarcon, M.A. Wnt/β-catenin signaling in Alzheimer's disease. *CNS Neurol. Disord. Drug Targets* **2014**, *13*, 745–754. [CrossRef]

120. Chenn, A. Wnt/β-catenin signaling in cerebral cortical development. *Organogenesis* **2008**, *4*, 76–80. [CrossRef]

121. Lukaszewicz, A.I.; Anderson, D.J. Cyclin D1 promotes neurogenesis in the developing spinal cord in a cell cycle-independent manner. *Proc. Natl. Acad. Sci. USA* **2011**, *108*, 11632–11637. [CrossRef] [PubMed]

122. Yan, J.; Zhang, H.; Yin, Y.; Li, J.; Tang, Y.; Purkayastha, S.; Li, L.; Cai, D. Obesity- and aging-induced excess of central transforming growth factor-beta potentiates diabetic development via an RNA stress response. *Nat. Med.* **2014**, *20*, 1001–1008. [CrossRef] [PubMed]

123. Salcedo-Tello, P.; Ortiz-Matamoros, A.; Arias, C. GSK3 Function in the Brain during Development, Neuronal Plasticity, and Neurodegeneration. *Int. J. Alzheimers Dis.* **2011**, *2011*, 189728. [CrossRef] [PubMed]

124. Steen, K.A.; Xu, H.; Bernlohr, D.A. FABP4/aP2 Regulates Macrophage Redox Signaling and Inflammasome Activation via Control of UCP2. *Mol. Cell. Biol.* **2017**, *37*, e00282-16. [CrossRef]

125. Van Steenwinckel, J.; Schang, A.L.; Krishnan, M.L.; Degos, V.; Delahaye-Duriez, A.; Bokobza, C.; Csaba, Z.; Verdonk, F.; Montane, A.; Sigaut, S.; et al. Decreased microglial Wnt/β-catenin signalling drives microglial pro-inflammatory activation in the developing brain. *Brain* **2019**, *142*, 3806–3833. [CrossRef]

126. Zhang, D.; Lu, Z.; Man, J.; Cui, K.; Fu, X.; Yu, L.; Gao, Y.; Liao, L.; Xiao, Q.; Guo, R.; et al. Wnt-3a alleviates neuroinflammation after ischemic stroke by modulating the responses of microglia/macrophages and astrocytes. *Int. Immunopharmacol.* **2019**, *75*, 105760. [CrossRef]

127. Tian, S.; Tan, S.; Jia, W.; Zhao, J.; Sun, X. Activation of Wnt/β-catenin signaling restores insulin sensitivity in insulin resistant neurons through transcriptional regulation of IRS-1. *J. Neurochem.* **2021**, *157*, 467–478. [CrossRef]

128. Song, D.; Zhang, X.; Chen, J.; Liu, X.; Xue, J.; Zhang, L.; Lan, X. Wnt canonical pathway activator TWS119 drives microglial anti-inflammatory activation and facilitates neurological recovery following experimental stroke. *J. Neuroinflammation* **2019**, *16*, 256. [CrossRef]

129. Cuevas-Diaz Duran, R.; Wei, H.; Wu, J.Q. Single-cell RNA-sequencing of the brain. *Clin. Transl. Med.* **2017**, *6*, 20. [CrossRef]

130. Keren-Shaul, H.; Spinrad, A.; Weiner, A.; Matcovitch-Natan, O.; Dvir-Szternfeld, R.; Ulland, T.K.; David, E.; Baruch, K.; Lara-Astaiso, D.; Toth, B.; et al. A Unique Microglia Type Associated with Restricting Development of Alzheimer's Disease. *Cell* **2017**, *169*, 1276–1290.e1217. [CrossRef]

131. Duffy, C.M.; Hofmeister, J.J.; Nixon, J.P.; Butterick, T.A. High fat diet increases cognitive decline and neuroinflammation in a model of orexin loss. *Neurobiol. Learn Mem.* **2019**, *157*, 41–47. [CrossRef]

132. Butterick, T.A.; Nixon, J.P.; Billington, C.J.; Kotz, C.M. Orexin A decreases lipid peroxidation and apoptosis in a novel hypothalamic cell model. *Neurosci. Lett.* **2012**, *524*, 30–34. [CrossRef]

133. Khan, A.; Ju, F.; Xie, W.; Tariq Hafeez, M.; Cheng, X.; Yang, Z.; Zhu, L.; Li, T.; Zhang, S. Transcriptomic analysis reveals differential activation of microglial genes after ischemic stroke in mice. *Neuroscience* **2017**, *348*, 212–227. [CrossRef]

134. Patro, R.; Duggal, G.; Love, M.I.; Irizarry, R.A.; Kingsford, C. Salmon provides fast and bias-aware quantification of transcript expression. *Nat. Methods* **2017**, *14*, 417–419. [CrossRef]

135. Yu, G.; Wang, L.G.; Han, Y.; He, Q.Y. clusterProfiler: An R package for comparing biological themes among gene clusters. *OMICS* **2012**, *16*, 284–287. [CrossRef]

136. Griss, J.; Viteri, G.; Sidiropoulos, K.; Nguyen, V.; Fabregat, A.; Hermjakob, H. ReactomeGSA-Efficient Multi-Omics Comparative Pathway Analysis. *Mol. Cell. Proteomics* **2020**, *19*, 2115–2125. [CrossRef]

137. Raudvere, U.; Kolberg, L.; Kuzmin, I.; Arak, T.; Adler, P.; Peterson, H.; Vilo, J. g:Profiler: A web server for functional enrichment analysis and conversions of gene lists (2019 update). *Nucleic Acids Res.* **2019**, *47*, W191–W198. [CrossRef]

138. McKenzie, A.T.; Wang, M.; Hauberg, M.E.; Fullard, J.F.; Kozlenkov, A.; Keenan, A.; Hurd, Y.L.; Dracheva, S.; Casaccia, P.; Roussos, P.; et al. Brain Cell Type Specific Gene Expression and Co-expression Network Architectures. *Sci. Rep.* **2018**, *8*, 8868. [CrossRef]

139. Mathys, H.; Davila-Velderrain, J.; Peng, Z.; Gao, F.; Mohammadi, S.; Young, J.Z.; Menon, M.; He, L.; Abdurrob, F.; Jiang, X.; et al. Single-cell transcriptomic analysis of Alzheimer's disease. *Nature* **2019**, *570*, 332–337. [CrossRef]

140. Cuddy, L.K.; Wani, W.Y.; Morella, M.L.; Pitcairn, C.; Tsutsumi, K.; Fredriksen, K.; Justman, C.J.; Grammatopoulos, T.N.; Belur, N.R.; Zunke, F.; et al. Stress-Induced Cellular Clearance Is Mediated by the SNARE Protein ykt6 and Disrupted by alpha-Synuclein. *Neuron* **2019**, *104*, 869–884.e11. [CrossRef]

141. Trychta, K.A.; Back, S.; Henderson, M.J.; Harvey, B.K. KDEL Receptors Are Differentially Regulated to Maintain the ER Proteome under Calcium Deficiency. *Cell Rep.* **2018**, *25*, 1829–1840.e26. [CrossRef]

142. Akama, T.O.; Nakagawa, H.; Wong, N.K.; Sutton-Smith, M.; Dell, A.; Morris, H.R.; Nakayama, J.; Nishimura, S.; Pai, A.; Moremen, K.W.; et al. Essential and mutually compensatory roles of α-mannosidase II and α-mannosidase IIx in N-glycan processing in vivo in mice. *Proc. Natl. Acad. Sci. USA* **2006**, *103*, 8983–8988. [CrossRef] [PubMed]

143. Jain Goyal, M.; Zhao, X.; Bozhinova, M.; Andrade-Lopez, K.; de Heus, C.; Schulze-Dramac, S.; Muller-McNicoll, M.; Klumperman, J.; Bethune, J. A paralog-specific role of COPI vesicles in the neuronal differentiation of mouse pluripotent cells. *Life Sci. Alliance* **2020**, *3*, e202000714. [CrossRef] [PubMed]

144. Sidjanin, D.J.; Park, A.K.; Ronchetti, A.; Martins, J.; Jackson, W.T. TBC1D20 mediates autophagy as a key regulator of autophagosome maturation. *Autophagy* **2016**, *12*, 1759–1775. [CrossRef] [PubMed]

145. Climer, L.K.; Dobretsov, M.; Lupashin, V. Defects in the COG complex and COG-related trafficking regulators affect neuronal Golgi function. *Front. Neurosci.* **2015**, *9*, 405. [CrossRef] [PubMed]

146. Zhao, J.; Wang, Y.; Xu, H.; Fu, Y.; Qian, T.; Bo, D.; Lu, Y.X.; Xiong, Y.; Wan, J.; Zhang, X.; et al. Dync1h1 Mutation Causes Proprioceptive Sensory Neuron Loss and Impaired Retrograde Axonal Transport of Dorsal Root Ganglion Neurons. *CNS Neurosci. Ther.* **2016**, *22*, 593–601. [CrossRef]

147. Schrotter, A.; Oberhaus, A.; Kolbe, K.; Seger, S.; Mastalski, T.; El Magraoui, F.; Hoffmann-Posorske, E.; Bohnert, M.; Deckert, J.; Braun, C.; et al. LMD proteomics provides evidence for hippocampus field-specific motor protein abundance changes with relevance to Alzheimer's disease. *Biochim. Biophys. Acta Proteins Proteom.* **2017**, *1865*, 703–714. [CrossRef]

148. Berchtold, N.C.; Coleman, P.D.; Cribbs, D.H.; Rogers, J.; Gillen, D.L.; Cotman, C.W. Synaptic genes are extensively downregulated across multiple brain regions in normal human aging and Alzheimer's disease. *Neurobiol. Aging* **2013**, *34*, 1653–1661. [CrossRef]

149. Wang, B.; Joo, J.H.; Mount, R.; Teubner, B.J.W.; Krenzer, A.; Ward, A.L.; Ichhaporia, V.P.; Adams, E.J.; Khoriaty, R.; Peters, S.T.; et al. The COPII cargo adapter SEC24C is essential for neuronal homeostasis. *J. Clin. Investig.* **2018**, *128*, 3319–3332. [CrossRef]

150. Li, S.; Yan, R.; Xu, J.; Zhao, S.; Ma, X.; Sun, Q.; Zhang, M.; Li, Y.; Liu, J.G.; Chen, L.; et al. A new type of ERGIC-ERES membrane contact mediated by TMED9 and SEC12 is required for autophagosome biogenesis. *Cell Res.* **2022**, *32*, 119–138. [CrossRef]

151. Naydenov, N.G.; Harris, G.; Brown, B.; Schaefer, K.L.; Das, S.K.; Fisher, P.B.; Ivanov, A.I. Loss of soluble N-ethylmaleimide-sensitive factor attachment protein alpha (αSNAP) induces epithelial cell apoptosis via down-regulation of Bcl-2 expression and disruption of the Golgi. *J. Biol. Chem.* **2012**, *287*, 5928–5941. [CrossRef]

152. Akila Parvathy Dharshini, S.; Taguchi, Y.H.; Michael Gromiha, M. Exploring the selective vulnerability in Alzheimer disease using tissue specific variant analysis. *Genomics* **2019**, *111*, 936–949. [CrossRef]

153. Liang, Z.S.; Cimino, I.; Yalcin, B.; Raghupathy, N.; Vancollie, V.E.; Ibarra-Soria, X.; Firth, H.V.; Rimmington, D.; Farooqi, I.S.; Lelliott, C.J.; et al. Trappc9 deficiency causes parent-of-origin dependent microcephaly and obesity. *PLoS Genet.* **2020**, *16*, e1008916. [CrossRef]

154. Helferich, A.M.; Brockmann, S.J.; Reinders, J.; Deshpande, D.; Holzmann, K.; Brenner, D.; Andersen, P.M.; Petri, S.; Thal, D.R.; Michaelis, J.; et al. Dysregulation of a novel miR-1825/TBCB/TUBA4A pathway in sporadic and familial ALS. *Cell Mol. Life Sci.* **2018**, *75*, 4301–4319. [CrossRef]

155. Ong, Y.S.; Tran, T.H.; Gounko, N.V.; Hong, W. TMEM115 is an integral membrane protein of the Golgi complex involved in retrograde transport. *J. Cell Sci.* **2014**, *127*, 2825–2839. [CrossRef]

156. Chornyy, S.; Parnis, A.; Shmoish, M.; Cassel, D. High abundance of ArfGAP1 found in the mossy fibers in hilus of the dentate gyrus region of the mouse brain. *PLoS ONE* **2017**, *12*, e0189659. [CrossRef]

157. Wang, X.; Shi, N.; Hui, M.; Jin, H.; Gao, S.; Zhou, Q.; Zhang, L.; Yan, M.; Shen, H. The Impact of β-1,4-Galactosyltransferase V on Microglial Function. *Front. Cell. Neurosci.* **2021**, *15*, 723308. [CrossRef]

158. Lin, C.Y.; Lai, H.L.; Chen, H.M.; Siew, J.J.; Hsiao, C.T.; Chang, H.C.; Liao, K.S.; Tsai, S.C.; Wu, C.Y.; Kitajima, K.; et al. Functional roles of ST8SIA3-mediated sialylation of striatal dopamine D2 and adenosine A2A receptors. *Transl. Psychiatry* **2019**, *9*, 209. [CrossRef]

159. Herring, B.E.; Shi, Y.; Suh, Y.H.; Zheng, C.Y.; Blankenship, S.M.; Roche, K.W.; Nicoll, R.A. Cornichon proteins determine the subunit composition of synaptic AMPA receptors. *Neuron* **2013**, *77*, 1083–1096. [CrossRef]

160. Sannerud, R.; Declerck, I.; Peric, A.; Raemaekers, T.; Menendez, G.; Zhou, L.; Veerle, B.; Coen, K.; Munck, S.; De Strooper, B.; et al. ADP ribosylation factor 6 (ARF6) controls amyloid precursor protein (APP) processing by mediating the endosomal sorting of BACE1. *Proc. Natl. Acad. Sci. USA* **2011**, *108*, E559–E568. [CrossRef]

161. Ziembik, M.A.; Bender, T.P.; Larner, J.M.; Brautigan, D.L. Functions of protein phosphatase-6 in NF-κB signaling and in lymphocytes. *Biochem. Soc. Trans.* **2017**, *45*, 693–701. [CrossRef] [PubMed]

162. Noel, J.; Ralph, G.S.; Pickard, L.; Williams, J.; Molnar, E.; Uney, J.B.; Collingridge, G.L.; Henley, J.M. Surface expression of AMPA receptors in hippocampal neurons is regulated by an NSF-dependent mechanism. *Neuron* **1999**, *23*, 365–376. [CrossRef] [PubMed]

163. Efimova, N.; Korobova, F.; Stankewich, M.C.; Moberly, A.H.; Stolz, D.B.; Wang, J.; Kashina, A.; Ma, M.; Svitkina, T. βIII Spectrin Is Necessary for Formation of the Constricted Neck of Dendritic Spines and Regulation of Synaptic Activity in Neurons. *J. Neurosci.* **2017**, *37*, 6442–6459. [CrossRef] [PubMed]

164. Gao, Z.H.; Seeling, J.M.; Hill, V.; Yochum, A.; Virshup, D.M. Casein kinase I phosphorylates and destabilizes the beta-catenin degradation complex. *Proc. Natl. Acad. Sci. USA* **2002**, *99*, 1182–1187. [CrossRef] [PubMed]

165. Bettencourt, C.; Foti, S.C.; Miki, Y.; Botia, J.; Chatterjee, A.; Warner, T.T.; Revesz, T.; Lashley, T.; Balazs, R.; Vire, E.; et al. White matter DNA methylation profiling reveals deregulation of HIP1, LMAN2, MOBP, and other loci in multiple system atrophy. *Acta Neuropathol.* **2020**, *139*, 135–156. [CrossRef]

166. Mendoza-Ferreira, N.; Karakaya, M.; Cengiz, N.; Beijer, D.; Brigatti, K.W.; Gonzaga-Jauregui, C.; Fuhrmann, N.; Holker, I.; Thelen, M.P.; Zetzsche, S.; et al. De Novo and Inherited Variants in GBF1 are Associated with Axonal Neuropathy Caused by Golgi Fragmentation. *Am. J. Hum. Genet.* **2020**, *107*, 763–777. [CrossRef]

167. Lu, X.; Zhang, D.; Shoji, H.; Duan, C.; Zhang, G.; Isaji, T.; Wang, Y.; Fukuda, T.; Gu, J. Deficiency of α1,6-fucosyltransferase promotes neuroinflammation by increasing the sensitivity of glial cells to inflammatory mediators. *Biochim. Biophys. Acta Gen. Subj.* **2019**, *1863*, 598–608. [CrossRef]

168. Rehfeld, A.; Plass, M.; Krogh, A.; Friis-Hansen, L. Alterations in polyadenylation and its implications for endocrine disease. *Front Endocrinol (Lausanne)* **2013**, *4*, 53. [CrossRef]

169. Alcott, C.E.; Yalamanchili, H.K.; Ji, P.; van der Heijden, M.E.; Saltzman, A.; Elrod, N.; Lin, A.; Leng, M.; Bhatt, B.; Hao, S.; et al. Partial loss of CFIm25 causes learning deficits and aberrant neuronal alternative polyadenylation. *eLife* **2020**, *9*. [CrossRef]

170. Gebhardt, A.; Habjan, M.; Benda, C.; Meiler, A.; Haas, D.A.; Hein, M.Y.; Mann, A.; Mann, M.; Habermann, B.; Pichlmair, A. mRNA export through an additional cap-binding complex consisting of NCBP1 and NCBP3. *Nat. Commun.* **2015**, *6*, 8192. [CrossRef]

171. Schonemann, L.; Kuhn, U.; Martin, G.; Schafer, P.; Gruber, A.R.; Keller, W.; Zavolan, M.; Wahle, E. Reconstitution of CPSF active in polyadenylation: Recognition of the polyadenylation signal by WDR33. *Genes Dev.* **2014**, *28*, 2381–2393. [CrossRef]

172. Cappell, K.M.; Larson, B.; Sciaky, N.; Whitehurst, A.W. Symplekin specifies mitotic fidelity by supporting microtubule dynamics. *Mol. Cell Biol.* **2010**, *30*, 5135–5144. [CrossRef]

173. Rosenthal, S.B.; Wang, H.; Shi, D.; Liu, C.; Abagyan, R.; McEvoy, L.K.; Chen, C.H. Mapping the gene network landscape of Alzheimer's disease through integrating genomics and transcriptomics. *PLoS Comput. Biol.* **2022**, *18*, e1009903. [CrossRef]

174. Ferre, C.A.; Thouard, A.; Betourne, A.; Le Dorze, A.L.; Belenguer, P.; Miquel, M.C.; Peyrin, J.M.; Gonzalez-Dunia, D.; Szelechowski, M. HSPA9/Mortalin mediates axo-protection and modulates mitochondrial dynamics in neurons. *Sci. Rep.* **2021**, *11*, 17705. [CrossRef]

175. Silva, P.N.; Furuya, T.K.; Braga, I.L.; Rasmussen, L.T.; Labio, R.W.; Bertolucci, P.H.; Chen, E.S.; Turecki, G.; Mechawar, N.; Payao, S.L.; et al. Analysis of HSPA8 and HSPA9 mRNA expression and promoter methylation in the brain and blood of Alzheimer's disease patients. *J. Alzheimer's Dis.* **2014**, *38*, 165–170. [CrossRef]

176. Jian, F.; Chen, D.; Chen, L.; Yan, C.; Lu, B.; Zhu, Y.; Chen, S.; Shi, A.; Chan, D.C.; Song, Z. Sam50 Regulates PINK1-Parkin-Mediated Mitophagy by Controlling PINK1 Stability and Mitochondrial Morphology. *Cell Rep.* **2018**, *23*, 2989–3005. [CrossRef]